AD-785 345

SHOCK TUBE OPERATION USING A COMPRESSION-HEATED DRIVER GAS

Richard C. Jenkins

Grumman Aerospace Corporation
Bethpage, New York

August 1974

Security Classification

DOCUMENT CONTROL DATA - R & D

(Security classification of title, body of abstract and indexing annotation must be entered when the overall report is classified)

1 ORIGINATING ACTIVITY *(Corporate author)*

Grumman Aerospace Corporation

2a. REPORT SECURITY CLASSIFICATION

AD 785345

2b. GROUP

3 REPORT TITLE

Shock Tube Operation Using a Compression Heated Driver Gas

4 DESCRIPTIVE NOTES *(Type of report and inclusive dates)*

Research Report

5 AUTHOR(S) *(First name, middle initial, last name)*

6 REPORT DATE	7a. TOTAL NO. OF PAGES	7b. NO. OF REFS
August 1974	68	0

8a. CONTRACT OR GRANT I	9a. ORIGINATOR'S REPORT NUMBER(S)
b. PROJECT NO N/A	RE 481
c.	9b. OTHER REPORT NO(S) *(Any other numbers that may be assigned this report)*
d.	

10 DISTRIBUTION STATEMENT

Approved for Public release; distribution unlimited.

11 SUPPLEMENTARY NOTES	12. SPONSORING MILITARY ACTIVITY
none	none

13. ABSTRACT

A high energy shock tube has been developed that employs free piston compression to energize the driver gas. The shock tube may be operated in either a constant volume or a constant pressure mode, depending upon whether or not the piston is brought to rest prior to diaphragm rupture. The constant volume mode was used to produce shock velocities up to 30,000 feet per second in helium and agron. The constant pressure mode was used to obtain tailored interface operation with helium driving argon at shock Mach numbers around 10. Analyses were developed for predicting piston behavior and shock tube operating characteristics in both modes. The results of these predictions are compared with our measurements. The shock tube performance calcualtions reveal some advantages of the constant pressure mode for tailored interface shock tube operation.

DD FORM 1 NOV 65 1473

Security Classification

Grumman Research Department Report RE-481

SHOCK TUBE OPERATION USING A COMPRESSION-HEATED DRIVER GAS

by

Richard C. Jenkins
Fluid Dynamics

August 1974

Approved by: Charles E. Mack, Jr.
Charles E. Mack, Jr.
Director of Research

1a

ACKNOWLEDGMENTS

The author appreciates the help provided by Fred Ellingson in the mechanical design of the apparatus as well as by Peter Greene, Alan Grillo, and George Lindsay during the experimental work.

ABSTRACT

A high energy shock tube has been developed that employs free-piston compression to energize the driver gas. The shock tube may be operated in either a constant volume or a constant pressure mode, depending upon whether or not the piston is brought to rest prior to diaphragm rupture. The constant volume mode was used to produce shock velocities up to 30,000 feet per second in helium and argon. The constant pressure mode was used to obtain tailored interface operation with helium driving argon at shock Mach numbers around 10. Analyses were developed for predicting piston behavior and shock tube operating characteristics in both modes. The results of these predictions are compared with our measurements. The shock tube performance calculations reveal some advantages of the constant pressure mode for tailored interface shock tube operation.

TABLE OF CONTENTS

LIST OF ILLUSTRATIONS

LIST OF SYMBOLS

a	local speed of sound
A	tube cross-sectional area
D	tube diameter
h	specific enthalpy
L	effective length of reservoir or pump tube
m	piston mass
M	flow Mach number
M_s	shock Mach number
M_{st}	shock Mach number for tailored interface operation
p	pressure in shock tube
P	pressure in reservoir or pump tube
P_{41}	P_4/P_1
t	time
u	piston velocity relative to tube; also used for local flow velocity in driven tube
u_s	shock velocity in driven tube
U	reference velocity
w_p	weight of piston
x	piston displacement from initial position
y	distance from piston face to effective endwall location
γ	isentropic exponent
λ_c	cutoff wavelength for microwave transmission in a tube
λ_f	free-space wavelength
λ_g	wavelength in a circular waveguide
ρ	gas density

Subscripts

1	reservoir gas conditions; also used for initial conditions in driven tube
2	pump tube gas conditions, also used for conditions behind shock in driven tube

01	initial conditions in reservoir gas
02	initial conditions in pump tube gas
3	local conditions behind interface in driven tube
3'	steady flow conditions downstream of orifice in driven tube
4	initial conditions in shock tube driver gas
5	conditions behind reflected shock in driven tube
r	conditions in pump tube gas at diaphragm rupture
f	conditions in pump tube gas at piston rebound

Superscripts

*	conditions at sonic point in a steady flow

I. INTRODUCTION

The free-piston compressor was developed to increase our shock tube energy capabilities and thus raise the velocity range of nozzle flow fields formed by the expansion of shock-heated gases. This compression device uses a single stroke of a pneumatically driven piston to heat and compress helium driver gas. Heating the driver gas enhances shock tube performance from two standpoints: first, the shock Mach number obtainable with a given initial diaphragm pressure ratio increases strongly with the driver gas temperature; second, the shock Mach number at which tailored interface operation can be achieved in a shock tunnel also increases as the driver gas temperature increases.

A compression-heated driver has several advantages over alternative driver heating methods, such as arc discharge or combustion. A significant advantage is that the free-piston compressor can be operated in two different modes. It can be used to develop either the conventional constant volume driver or else the less familiar constant pressure driver. In the former mode of operation a compression-heated driver can produce much higher shock Mach numbers than a combustion driver, and its performance characteristics are comparable with an arc-heated driver (Ref. 1). This mode is most useful for operation at shock Mach numbers above 20 when testing time is not a problem.

The tube may be operated in the constant pressure mode when it is desired to produce longer testing times by the tailored interface technique. Shock Mach numbers are lower than for the constant volume case, but testing time is greatly increased because this technique prevents the reflected shock wave from interacting with the interface between the driver and the driven

gases. Tailoring can be achieved at shock Mach numbers considerably higher than with combustion heating and comparable with arc heating. This performance is obtained by allowing the diaphragm to rupture while the piston is in motion (Refs. 2-4). The compression-heated driver requires considerably less energy for its operation than other techniques. Further advantages compared to arc heating are the lack of electromagnetic interference and considerably lower contamination levels.

Shock tube operation in the constant volume mode can be analyzed using relations presented in Ref. 5. In the constant pressure mode, shock tube operation is complicated by a steady-state expansion of the driver gas and requires a different type of analysis. Two separate analyses are developed to describe the different piston velocities required to produce these two modes of operation.

II. DESCRIPTION OF OPERATION

A sketch of the free-piston compressor, shock tube, and associated equipment is shown in Fig. 1. The tube assembly consists of three separate sections: the reservoir, the compression tube, and the driven tube. Together, the reservoir and the compression tube are referred to as the free-piston compressor. The compressor section produces a high pressure driver gas that ruptures a metal diaphragm and drives a high velocity shock wave through the gas in the driven tube. While the compressor is rigidly attached to the pump tube at the diaphragm station by a high pressure collar, the compressor can be operated independently of the driven tube by inserting a thick aluminum plug in place of the diaphragm. This type of operation is referred to as closed tube operation.

To operate the compressor, the piston is mechanically restrained at its initial position as the gas pressure in the reservoir behind it is increased. When the piston is released it moves rapidly through the compression tube for a distance of approximately 11 feet until it is brought to rest by the compressed gas trapped ahead of it. The distance traveled by the piston during the compression stroke depends on the initial pressure ratio across it. The time required for the compression stroke is determined by the initial reservoir pressure and the piston mass.

The piston behavior close to the end of the stroke depends on what type of run is made. For a closed tube run the piston rebounds back through the compression tube after stopping at the closed end. For shock tube type operation the compressed gas ruptures the diaphragm and the piston comes to rest at the diaphragm station. Two modes of shock tube operation are used, the difference between modes being caused by differences in the piston motion close to the end of

the stroke. For one mode of operation, designated a constant volume driver, the piston comes to rest just as the diaphragm breaks. For the second mode, designated a constant pressure mode, the piston is still moving at high velocity when the diaphragm breaks, and thereafter the piston decelerates as it approaches and strikes the end wall at relatively low velocity. These two modes of shock tube driver operation are described in greater detail below.

A detailed investigation of the flow conditions in the driven tube was necessary to determine the capabilities of these two different driver modes. In a conventional shock tube (constant volume driver mode), when the diaphragm ruptures, a shock wave propagates through the driven tube while simultaneously an expansion wave moves back through the driver. An interface that separates the gases that were originally in the driver and driven sections closely follows the shock wave. The expansion wave reflects from the rear wall of the driver back into the driven tube; eventually it overtakes the interface and shock wave (if the driven tube is long enough) because its velocity is greater. When the shock wave reflects from the closed end of the driven tube it moves back toward the oncoming interface, leaving a region of hot, stagnant driven tube gas near the end wall. The region near the end wall is referred to as the reflected zone. If the reflected shock wave passes through the interface without generating a disturbance in the reflected zone, the shock tube is said to be operating under tailored interface conditions.

At the end of the pump tube, adjacent to the diaphragm, there is a short channel (Fig. 2) with the same ID as that of the driven tube. When used as a constant-volume shock tube driver, this channel becomes the driver section, and the piston comes to rest close

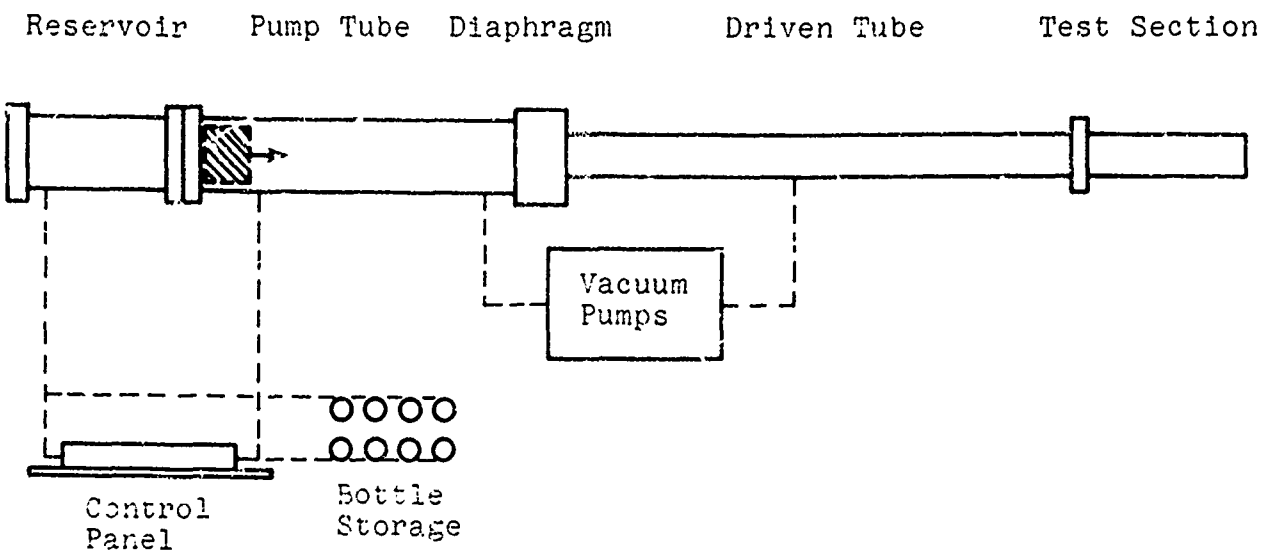

Fig. 1 Sketch of Free-Piston Shock Tube

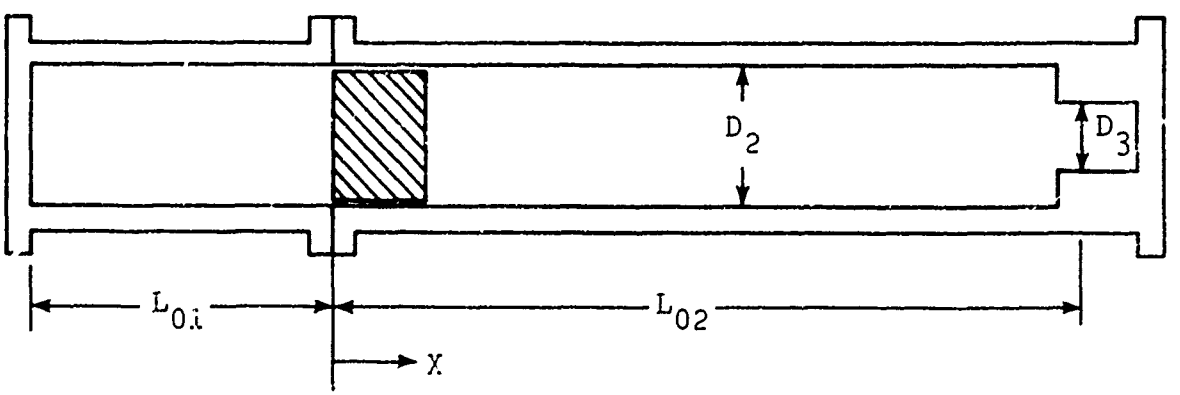

L_{01} = 4.174 ft D_2 = 10.6 in.

L_{02} = 11.551 ft D_3 = 5.2 in.

X_{MAX} = 11.359 ft W_p = 38 lb

Fig. 2 Schematic Diagram of Compressor

to the channel face just as the diaphragm breaks. A spike mounted on the front of the piston breaks the diaphragm when the piston reaches the end of the stroke. This mode of operation provides the maximum compression ratio and thus the highest possible driver gas temperature at diaphragm rupture. Although the driver section is only about one foot long, this length is sufficient if the shock velocity is high enough so that the reflected expansion head arrives at the end wall of the driven tube a few hundred microseconds later than the incident shock. Operation in this mode provides extremely high energy gas in the reflected zone of the driven tube for a very short time period.

Longer duration nozzle flows can be obtained by delaying the arrival of disturbances in the reflected shock zone. Two changes must be made to extend the duration of the steady conditions significantly. First, disturbances generated by the reflected shock passing through the interface are suppressed by operating the driven tube under tailored interface conditions. Second, the arrival of the reflected expansion head must be delayed a few milliseconds. This latter change can be accomplished by operation in a constant pressure mode. The diaphragm is allowed to break before the piston reaches the end of its stroke, when the piston is moving rapidly enough for its motion to compensate for driver gas flow into the driven tube. The movement of the piston at and following diaphragm rupture suppresses the formation of an expansion wave for several milliseconds until the piston comes to rest at the compressor end wall.

III. ANALYSIS OF PISTON MOTION

A. Closed Tube

To analyze the piston motion in a closed tube we used an analysis similar to that developed by Roffe (Ref. 6). This relatively simple analysis provides a partial description of piston behavior during shock tube operation since the motion of the piston up to the time of diaphragm rupture is the same as if the tube were closed.

The reservoir and pump tube gases are assumed to undergo a quasi-steady, isentropic expansion and compression. This assumption imposes certain constraints on piston motion. The compression stroke must be rapid enough to neglect heat transfer to the walls but slow enough to avoid the influence of unsteady wave processes in the gases. In addition, friction forces on the piston must be negligible compared to pressure forces and the piston rings must prevent any gas leakage past the piston. A frame of reference was selected that is stationary with respect to the tube assembly, assuming that the piston mass is very small compared to the mass of the tube assembly so that acceleration of the latter can be neglected.

The schematic diagram (Fig. 2) shows only the reservoir and pump tube. Let the subscript 1 denote conditions behind the piston and 2 denote conditions ahead of the piston. The additional subscript 0 denotes initial conditions before piston release. The quantity L_{02} represents the effective length of the pump tube; that is, the length of a completely cylindrical pump tube with the same volume. L_{01} is the effective reservoir length. The distance x represents the displacement of the piston from its initial location.

The pressure ahead of the piston is given by

$$P_2 = P_{02}\left(\frac{L_{02}}{L_{02} - x}\right)^{\gamma_2} , \qquad (1)$$

where P_{02} is the initial pressure in the pump tube and γ_2 is the isentropic exponent. Similarly, for the pressure behind the piston

$$P_1 = P_{01}\left(\frac{L_{01}}{L_{02} + x}\right)^{\gamma_1} . \qquad (2)$$

Then the equation of motion for a piston with mass m and cross-sectional area A is

$$\frac{m}{A}\frac{d^2x}{dt^2} = P_{01}\left(\frac{L_{01}}{L_{01} + x}\right)^{\gamma_1} - P_{02}\left(\frac{L_{02}}{L_{02} - x}\right)^{\gamma_2} . \qquad (3)$$

Integrating with respect to time and applying the condition that $u = 0$ for $t = 0$, the following expression can be found for piston velocity as a function of displacement

$$\frac{mu^2}{2A} = \frac{P_{02}L_{02}}{(\gamma_2 - 1)}\left[1 - \left(\frac{L_{02}}{L_{02} - x}\right)^{\gamma_2 - 1}\right] - \frac{P_{01}L_{01}}{(\gamma_1 - 1)}\left[\left(\frac{L_{01}}{L_{01} + x}\right)^{\gamma_1 - 1} - 1\right] . \qquad (4)$$

Figure 3 shows the piston velocities predicted by Eq. (4) for a given initial reservoir pressure and several different initial pump tube pressures. As the initial pump tube pressure is decreased, the shape of the curves change and the point of piston rebound moves further downstream. The maximum displacement can be

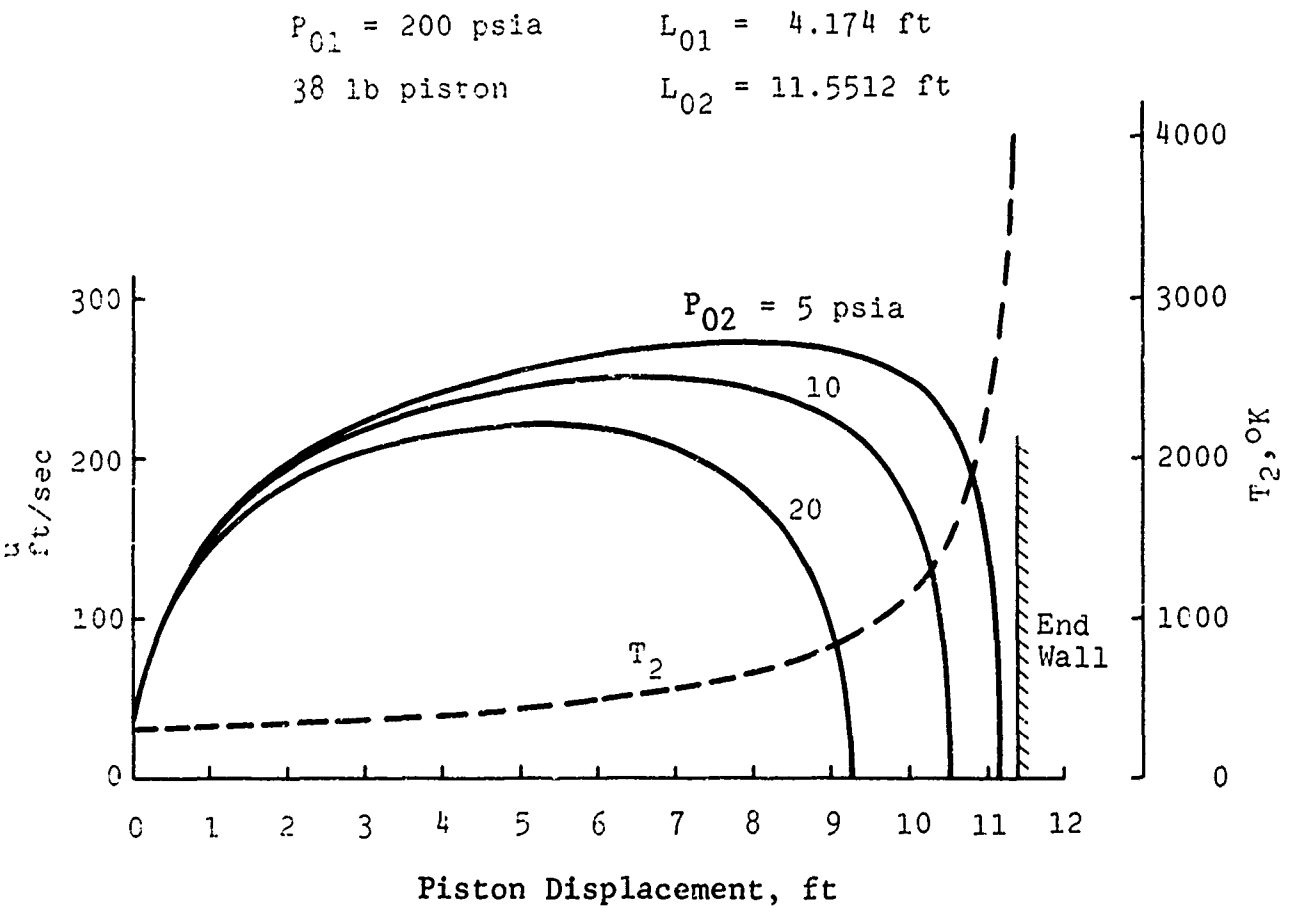

Fig. 3 Piston Velocity vs. Displacement

found from Eq. (4) by assuming $u = 0$. Results show that the maximum displacement at rebound is independent of piston mass and for a given geometry depends only on the initial pressure ratio across the piston. However, the stroke time does depend on piston mass since for given P_{01} and P_{02} the velocity at any point is inversely proportional to the square root of piston mass.

The shape of the curves in Fig. 3 illustrates why, for a given P_{01}, a higher peak pressure is developed at the end of the stroke by using a lower value of P_{02}. Consider the maximum velocity point on the lower curve which assumes an initial pump tube pressure of 20 psi. At that location, $P_1 = P_2$. The piston requires a certain average product of force times distance to reach that velocity, and it requires the same average value of force times distance to stop it at the rebound point. Now consider the upper curve where the initial pump tube pressure is assumed to be 5 psi. There is an even higher maximum velocity later in the stroke compared to the 20 psi case, yet the stopping distance is much shorter. For this curve the pressure developed in the compressed gas is extremely high, much higher than the initial reservoir pressure P_{01}. This behavior is referred to as pressure amplification and is one of the advantages of piston compression for driving a shock tube. The diaphragm can be broken with a high energy gas pulse that has a pressure far beyond the initial pressure anywhere in the system. In fact, care must be taken in setting the initial conditions so as not to choose too low a value of P_{02} and drive the peak pressure above the 10,000 psi design rating of the high pressure collar.

B. Constant Volume Driver

The closed tube analysis is used to describe the piston behavior and to calculate the driver gas conditions when the piston tube is operated as a constant volume shock tube driver. When this mode is used it is generally desired to have the highest possible driver temperature. This results from a maximum stroke length. The initial pressure ratio, P_{01}/P_{02}, required to obtain a desired stroke length can be found from Eq. (4). The level of P_{02} required to obtain a given diaphragm rupture pressure can be found from Eq. (1) using the stroke length. Thus the initial conditions are specified by the desired driver conditions, and, if the stroke time is of interest, it can be approximated by graphic integration of an appropriate plot of u versus x.

For an isentropic compression the temperature of the gas ahead of the piston is given by

$$T_2 = T_{02}\left(\frac{L_{02}}{L_{02} - x}\right)^{\gamma_2 - 1} . \qquad (5)$$

This relation shows that the temperature is only a function of the volumetric compression ratio and the isentropic exponent γ_2. A dashed curve showing this relation between T_2 and x appears in Fig. 3. Note the rapid temperature rise as the piston approaches the maximum displacement. For a full stroke, with the piston face stopping right at the entrance to the driver section, isentropic theory predicts a helium driver temperature of about 4000°K. The pressure variation follows the same general behavior, with P_2 increasing very rapidly near the end of the stroke.

For shock tube operation the conditions in the piston-compressed gas at diaphragm rupture represent the shock tube driver gas conditions.

The notation shown in Fig. 2 is used to describe compressor operation, and the notation in the appendix is used to describe shock tube operation. At diaphragm rupture the compressed gas properties P_2, T_2, and γ_2 become the driver conditions P_4, T_4, and γ_4.

C. Constant Pressure Driver

A description of piston behavior needed to produce the constant pressure mode requires a more complex analysis. The diaphragm is allowed to break before the piston reaches the end of its stroke. An orifice plate (Fig. 4) must be added at the diaphragm station to restrict the flow of driver gas into the driven tube. The analysis of piston motion after diaphragm breakage follows that developed by Stalker (Ref. 3). It is used to determine the initial pressure ratio and diaphragm rupture point required to maintain driver gas conditions approximately constant for a few milliseconds after diaphragm rupture. The analysis assumes steady-state, isentropic flow of the driver gas with sonic conditions at the exit orifice.

Let the subscript r denote the compressed gas conditions at diaphragm rupture, and define a reference velocity U_r as the piston velocity that would be required at diaphragm rupture to produce disturbance-free driver conditions. The actual piston velocity at rupture is denoted by u_r. The one dimensional mass flow equations can be used to relate U_r to the driver gas conditions and the ratio of sonic point area to pump tube area. For a perfect gas

$$U_r = \frac{\rho_r^*}{\rho_r} \sqrt{\frac{T_r^*}{T_r}}\, a_r \, \frac{A^*}{A} \quad ,$$

where the asterisk denotes properties at the sonic point and a_r is the speed of sound in the compressed gas at diaphragm rupture.

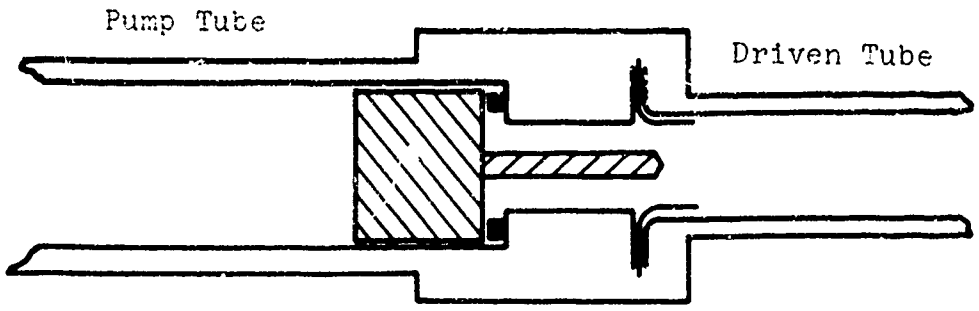

a) Constant Volume Mode

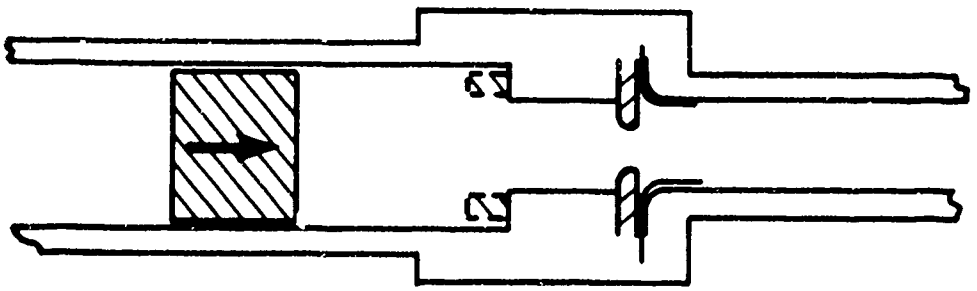

b) Constant Pressure Mode

Fig. 4. Compressor Operating Modes

When the area ratio is specified, the density and temperature ratios can be evaluated, and U_r becomes only a function of compressed gas temperature The reference velocity U_r is plotted versus temperature in Fig. 5 for a helium driver. The upper curve was developed by assuming A^*/A was the area ratio between the pump tube and driven tube. Since the shock Mach number for tailored interface operation (designated M_{st}) is determined by the temperature of the helium driver gas, approximate values of M_{st} in air have been indicated along the temperature coordinate.

By choosing u_r somewhat greater than U_r, the driver gas pressure can be made to increase slightly after diaphragm rupture and then decrease monotonically as the piston comes to rest. For the driver pressure to remain approximately constant for a few milliseconds, it is necessary to have u_r about 50 percent greater than U_r. Furthermore, the maximum piston velocity before rupture must be considerably greater than u_r. From the upper curve in Fig. 5 it is apparent that at high M_{st} maximum piston velocities of 2000 feet/second would be required if the helium driver gas were allowed to flow directly into the driven tube. This range of piston velocity is impractical. By installing an orifice in the driver section adjacent to the diaphragm, the required piston velocity can be lowered to a more reasonable range. The lower two curves in Fig. 5 show the variation of U_r with T_{2r} for a 2-inch or 3-inch diameter orifice plate installed at the diaphragm station. A 3-inch diameter orifice plate would reduce the maximum piston velocity to about 600 feet/second for tailoring at high M_s. This velocity range can be produced using an 800 psi initial reservoir pressure. Driver performance is affected by the area expansion downstream of the orifice, and one finds the prediction of shock tube performance characteristics more complex because of it.

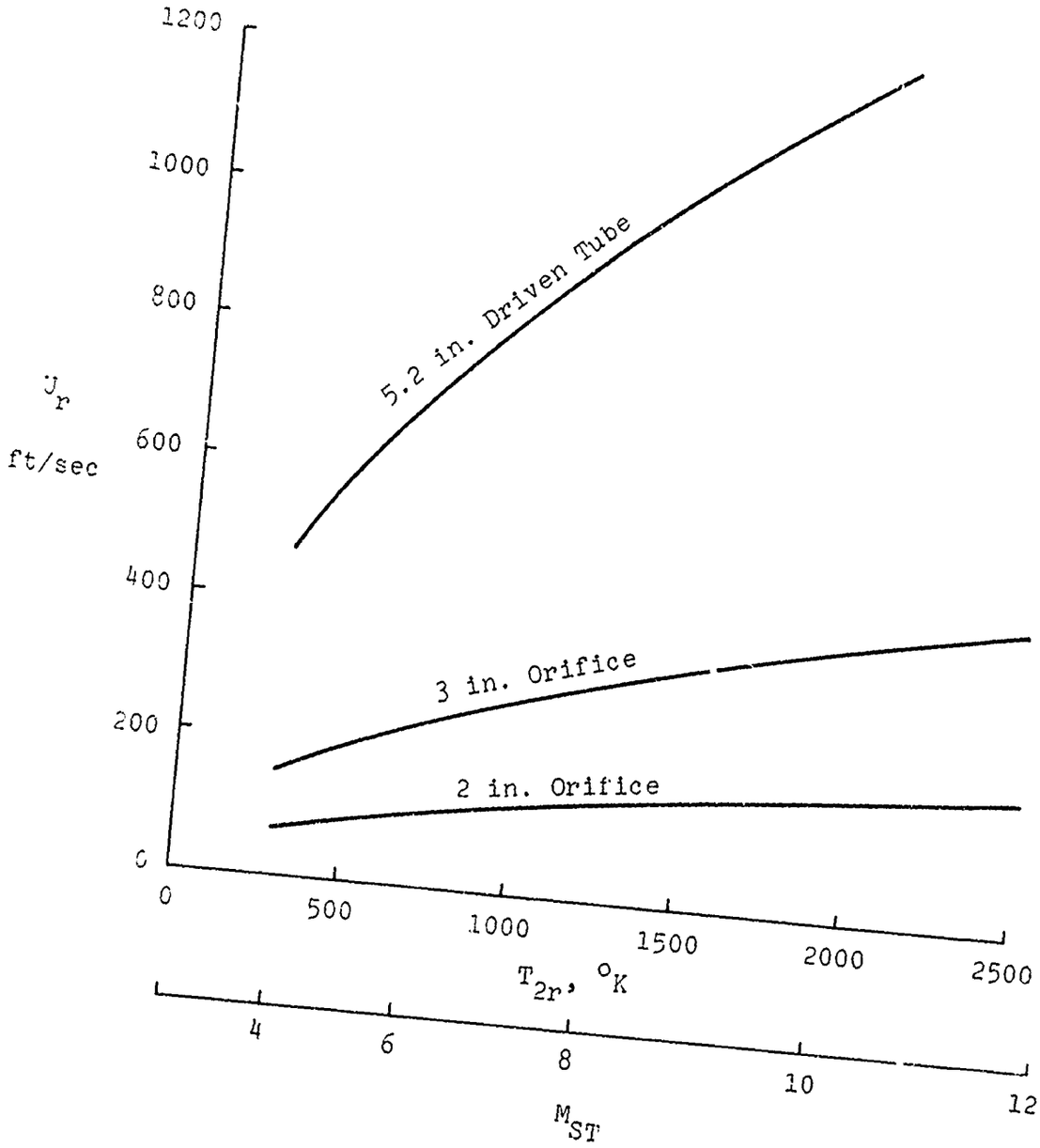

Fig. 5 Reference Velocity vs Temperature

To determine the variation in compressed gas conditions ahead of the piston after diaphragm rupture, let

$$y = L_{02} - x \quad .$$

For isentropic flow between the pump tube and the orifice, Stalker (Ref. 3) has shown that the motion of the piston can be related to the mass flow through the orifice with the equation

$$\frac{d}{dt}(\rho y) = - \left(\frac{\rho}{\rho_r}\right)^{\frac{\gamma+1}{2}} \rho_r U_r \quad . \tag{6}$$

The equation of motion of the piston is given by

$$\frac{du}{dt} = - \frac{A}{m} (P - P_1) \quad , \tag{7}$$

where

$$u = - \frac{dy}{dt} \quad .$$

If expansion or compression of the gas ahead of the piston is isentropic, then

$$\frac{P}{P_r} = \left(\frac{\rho}{\rho_r}\right)^{\gamma} \quad . \tag{8}$$

The pressure behind the piston is given by

$$P_1 = P_{01}\left(\frac{L_{01}}{L_{01} + L_{02} - y}\right)^{\gamma_1} \quad . \tag{9}$$

Equations (6) through (9) can be used to determine the variation in driver gas conditions and the piston motion as functions of time after the diaphragm has opened. These equations were programmed and a number of computer runs were made to determine the initial

conditions and diaphragm rupture point required to produce specified driver conditions. For an assumed diaphragm rupture point, the closed-tube equations provided the driver gas conditions required to start the calculations at diaphragm rupture.

Figure 6 shows a plot of piston velocity after diaphragm rupture versus distance from the end wall obtained from one computer run made for a 2-inch diameter orifice. The computer program also tabulates p/p_r and T/T_r as functions of time after diaphragm rupture corresponding to each curve. The curves in Fig. 6 were produced by assuming the same initial reservoir and pump tube pressures and choosing five different diaphragm rupture points. Piston impact against the end wall was predicted for each assumed rupture point. The impact velocity decreases as the diaphragm rupture point is moved forward until conditions are such that a partial rebound occurs; that is, the piston stops close to the end, rebounds slightly, and then reaccelerates into the end. For the initial pressures chosen for Fig. 6, a diaphragm rupture point of x_r = 11.25 feet would yield an impact velocity of 40 feet/second. The corresponding tabulation of pressure and temperature show the driver conditions would vary by less than 10 percent for 1.5 milliseconds after diaphragm rupture, and tailored-interface operation should be possible at M_{st} = 12.

A number of computer calculations were carried out for various initial conditions and the results plotted on a CRT display terminal for rapid analysis. For a 2-inch diameter orifice, the lowest impact velocity predicted for any combination of initial conditions and diaphragm rupture points was 20 feet/second. Impact velocities less than 50/second were predicted for a wide range of driver gas conditions. For a 3-inch diameter orifice the required piston velocities were higher, the time duration of relatively constant pressure was less, driver gas temperatures were higher, and piston impact

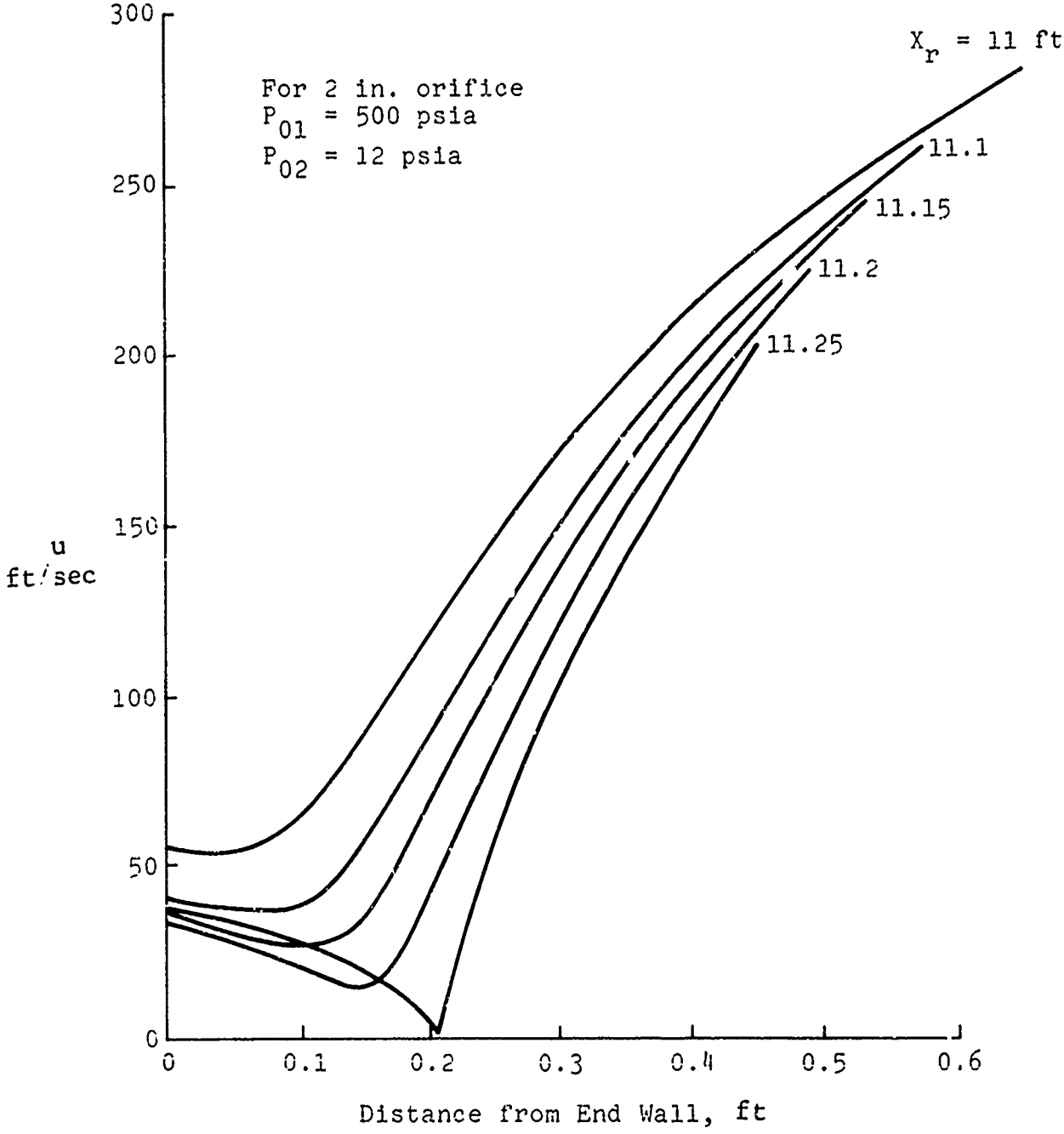

Fig. 6 Piston Velocity After Diaphragm Rupture

velocity was also generally higher. The duration of approximately steady driver conditions was found to decrease as driver temperature increased because the required piston velocity was higher and the diaphragm rupture point was closer to the end wall. This decrease in steady P_4 duration with T_4 was observed for both orifice diameters, indicating that the maximum duration of steady conditions in the reflected zone must decrease as M_{st} is increased.

IV. EXPERIMENTAL EQUIPMENT AND TECHNIQUES

A. Tube Assembly

The reservoir is approximately 4 feet long; the pump tube, 12 feet long. Both have a 10.6-inch ID and 12-inch OD. These sections were designed for 2000 psi and hydrostatically tested to 3000 psi. The diaphragm end of the pump tube is limited to a maximum impulse pressure of approximately 10,000 psi. The driven tube is 20 feet long with a 5.2-inch ID. Each of these sections of the tube assembly are independently evacuated, purged, and filled by the gas handling system prior to operation.

The piston, shown in Fig. 7, is a hollow aluminum shell with a central steel tang. Before the piston is released, an "O"-ring on the back of the piston forms a gas seal between the reservoir and the pump tube. The piston is mechanically restrained at its initial position by a hollow bar that is anchored to the rear wall of the reservoir. When the piston is set in its initial position, the steel tang on the piston fits inside this bar and is spread outward by a centerbody within the bar, restraining the piston from forward motion. With a high pressure in the reservoir, the piston is launched by withdrawing the centerbody. This release mechanism has performed satisfactorily at reservoir pressures up to 400 psi, and should be capable of operation up to 1000 psi.

An important consideration in compressor design was to maintain low contamination levels in the compressed gas to prevent driver gas contaminants from coating the driven tube walls. This requirement was partially satisfied by avoiding the use of lubricants on the pump tube walls. Two seal rings mounted on the piston contact the pump tube walls and prevent leakage past the piston

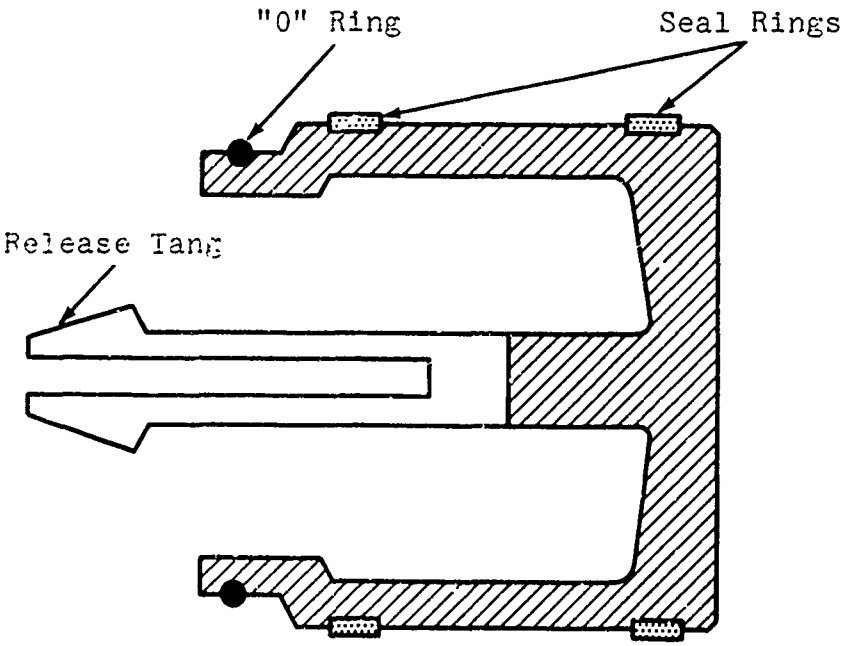

Fig. 7 Hollow Aluminum Piston

during the compression stroke. In the initial work pure teflon rings were used. Because of rapid ring wear we changed to a composite ring material (20 percent Fibreglas and 80 percent Teflon). The thermal expansion of this material is high enough to machine the rings to the desired size and shrink-fit them on the hollow piston. The ring OD was cut 0.005-inch smaller than the pump tube ID; after about 100 runs the ring fit was still close enough to show no change in compression characteristics. The primary source of ring wear was found to be local erosion of the forward ring where it is exposed to the hot compressed gas.

The piston weighs 38 pounds, and the reservoir, pump tube, and driven tube together weigh approximately two tons. The tube assembly recoils in response to piston motion. Rather than attempt to restrain this motion the entire tube assembly is mounted on rollers so that it is free to recoil. For safety, shock absorbers were installed to restrain axial movement of the tube assembly beyond three inches from its initial position. These shock absorbers have not engaged during any of the tests described, since the tube recoil distance is only $1\frac{1}{4}$-inches for a full compression stroke of the piston (approximately an 11 foot stroke length).

The time duration of this recoil is between 40 and 100 milliseconds, depending on reservoir pressure, and the tube assembly comes to rest at its new location just after diaphragm rupture. However, if the compressor is operated with a solid plug at the diaphragm station (for investigation of piston behavior), this initial $1\frac{1}{4}$-inch recoil is followed by a series of damped tube oscillations that last until the piston finally comes to rest. The tube assembly responds to these piston oscillations by moving axially so that the center of mass of the combined system remains stationary.

The most critical design problem in the compressor involved piston impact against the end wall. The piston could always be brought to rest before the end wall, but a partial rebound could then be followed by reacceleration of the piston into the end by the expanded reservoir gas. For our early work a conservative approach to this problem was taken as a safety precaution. The end wall was covered with a hollow cylinder of crushable aluminum honeycomb. This material, manufactured by Hexcel Corp. under the trade name Tubecore, had a uniform crush force over three quarters of its length. The thickness of this material was chosen so as to permit an impact velocity up to 120 feet/second.

Operation in the constant volume mode led to impact velocities in the range of only a few feet/second, permitting a given piece of honeycomb to be used for many runs. Its main disadvantages were that its cellular structure soaked up considerable heat from the compressed driver gas, and the binder material used in its construction degraded at high temperature and provided a severe contamination problem. Because of the low piston velocities we discarded the honeycomb and used nylon impact discs mounted on the end wall. Contamination from thermal degradation of nylon was quite low, and the impact was mild enough to use the discs a dozen times before replacement.

Operation in the constant pressure mode leads to high impact velocity. Nylon was not used because replacement would have been required on every run, and the time lost in tube disassembly would have been prohibitive. The first several runs in this mode were made using honeycomb until a more convenient impact mechanism could be built. This mechanism consists of eight pneumatic plungers that were built into the end wall. Each plunger has a two inch internal

diameter and a two inch stroke. Preloading the plunger cavities with helium to a pressure of 1000 psi makes this device usable up to impact velocities of 120 feet/second. Its primary advantage is that it resets itself, and frequent tube disassembly is not required. Because this device provides a resiliant type of impact, the piston energy at the end of the stroke is dissipated by multiple impact.

Control of diaphragm break pressure was critical during constant pressure operation. The break pressure of a diaphragm of given thickness was varied by changing the depth of a pair of crossed lines that are cut (or scribed) on one surface. The variation of rupture pressure with scribe depth for a given diaphragm thickness was determined early in this investigation by running a series of static diaphragm burst tests. However, we felt that in this early work the slow buildup in pressure prior to rupture did not adequately simulate the pulse-type pressure rise before diaphragm rupture during compressor operation, and that a diaphragm scribed to a given depth might break at a higher pressure under dynamic pressure loading than it would under static loading.

To resolve this question a short series of dynamic break tests were performed with the compressor operating in a modified closed tube mode. We used a plug just downstream of the diaphragms to limit the downstream volume of the driven tube to less than 0.1 cubic foot so that the high pressure gas cushion ahead of the piston would not be diminished and allow the piston to strike the end wall. These dynamic break tests produced the same rapid pressure rise prior to rupture that occurs during actual compressor operation. The variation of break pressure with scribe depth found from these tests was about 10 percent higher in pressure level

than that obtained from the static break tests. The piston stroke time was nominally 35 milliseconds, but most of the pressure rise occurred 5 milliseconds prior to diaphragm rupture.

All three sections of the tube assembly were evacuated and purged prior to shock tube operation. Special consideration was given to the driven tube to obtain high gas purity at the lower levels of p_1. An ultimate tube pressure of 200 microns was obtained using a mechanical pump, and long term leak tests showed a leak rate of 5 microns per hour. The shock tube was generally run within 20 minutes after purging and setting the driven tube pressure at the desired p_1.

B. Instrumentation

The initial pressure P_{01} and P_{02} were measured with Bourdon tube gauges. During piston motion the pressure in the pump tube ahead of the piston was measured with two piezoelectric gauges (Type 603H, Kistler Manufacturing Corp.) that were flush-mounted in the driver section close to the diaphragm station. The gauges were coated with a thin layer of thermal insulation to minimize error caused by heat transfer during the compression stroke. Either H-film tape ($\frac{1}{2}$-mil thick) or an elastic type of contact cement were found to provide adequate thermal insulation.

Measurements of maximum piston velocity were made using a microwave technique to check the values predicted by Eq. (4). The pump tube was used as a circular waveguide, excited by a loop antenna located inside the reservoir. An oscillator was used to drive the antenna at 835 MHz, a frequency chosen to suppress transmission in modes other than the lowest frequency TE_{11} mode. The signal from the antenna, received by a diode through a directional coupler, was displayed on an oscilloscope.

Motion of the piston produced oscillations in the antenna signal level corresponding to changes in the standing wave pattern behind the piston. Sharply defined peaks appeared every time the piston moved a distance equal to half the guide wavelength, given by

$$\lambda_g = \frac{\lambda_f}{\sqrt{1 - \left(\frac{\lambda_f}{\lambda_c}\right)^2}} \quad . \tag{10}$$

where λ_f is the free space wavelength of the applied signal and λ_c is the cutoff wavelength of the mode propagated in the waveguide. For a circular waveguide with diameter D, the cutoff wavelength of the TE_{11} mode can be found from

$$\lambda_c = 1.706\ D \quad .$$

The piston was mechanically moved through the tube, and the displacement corresponding to peaks in the output signal was found to be 11.31 inches, which is half the guide wavelength predicted by Eq. (10). During pump tube operation the piston velocity was found by dividing this distance by the measured time interval between signal peaks. The spatial resolution of such measurements is poor because of the large piston displacement between signal peaks, so details of local velocity could not be resolved close to the end of the stroke where the acceleration was high. For measurements of maximum piston velocity, however, this approach was adequate.

A more convenient method of measuring piston velocity was developed using the recoil of the tube assembly. A constant voltage was applied to a thin-film linear potentiometer that was set up to monitor movement of the rear reservoir flange relative the the rear

support stand. The voltage on the sliding arm was displayed on an oscilloscope. The piston and the tube assembly move relative to each other in such a way that the center of mass of the combined system remains stationary. At any time after piston launch, the displacement and velocity of the piston are proportional to the displacement and velocity of the tube assembly. The proportionality constant is the ratio of piston mass to the mass of the tube assembly.

Unlike the microwave technique, this recoil method of velocity measurement has excellent resolution and thus can provide an accurate measurement in regions of high piston acceleration. It is particularly useful during constant pressure driver operation for determining piston behavior near the end wall and for measuring piston velocity at impact. Measurements of piston velocity obtained with microwave and with tube recoil techniques were not directly compared, but the investigations did verify that measurements of maximum piston velocity obtained with both methods agreed with theoretical predictions.

Accurate measurements of stroke length were obtained during closed tube runs not only to compare compressor performance against theory but also to be completely sure of the location of the point of piston reversal before breaking a diaphragm at new operating conditions. Two methods of measuring the reversal point were used. When the rebound point was far from the compressor end wall, an electrical contact gauge mounted on an adjustable arm extending from the diaphragm plug was used to signal arrival of the piston face at a known location. At higher compression ratio this technique was not satisfactory because high pressures and temperatures caused premature operation of the switch. Measurements of piston

rebound close to the end wall were made with deformable copper tabs mounted on the wall.

Measurement of piston displacement at reversal x_f and maximum pressure P_{2f} provides an indirect measure of temperature at the end of the stroke. The temperature at rebound can be found from the ideal gas equation of state

$$T_{2f} = T_{02}\left(\frac{P_{2f}}{P_{02}}\right)\left(\frac{L_{02} - x_f}{L_{02}}\right) \quad . \tag{11}$$

This expression is similar to Eq. (5) except that it does not assume that the driver gas compression is isentropic.

Three types of pressure gauges were used for driven tube measurements. Bourdon type gauges were used to control tube pressure during vacuum purging and to set initial p_1 level before a run. A thermocouple gauge was used to determine ultimate vacuum level and leak rate. Flush-mounted piezoelectric gauges were used to measure pressures behind incident and reflected shock waves, p_2 and p_5. In this high temperature environment an elastic adhesive proved to be a better thermal insulation for the gauges than any other method attempted.

Two techniques were used for measuring shock velocity in the driven tube. Piezoelectric gauges near the closed end of the driven tube provided measurement of time of arrival of the shock at locations spaced axially 3.46 feet apart. Thus the incident shock velocity could be found close to the point of shock reflection using some of the gauges used to determine pressure behavior in the reflected zone. In addition, the shock velocity was measured throughout the driven tube using the same microwave technique developed for piston velocity measurement. In this case the

driven tube walls were excited in the TE_{11} mode using a 1.7 KMHz signal from a circular antenna located on the closed end of the driven tube. There was sufficient ionization behind the incident shock during almost all our tests to obtain a measurable signal throughout the tube. This measurement was found to give excellent resolution because of sharp resonance peaks found in the signal for every 5.80-inch movement of the shock wave.

V. EVALUATION OF EXPERIMENTAL RESULTS

A. Closed Tube

The purpose of the first series of closed tube experiments was to evaluate the accuracy of our isentropic analysis. Microwave measurements of piston velocity verified that the peak velocities predicted by theory were actually attained, at least to within the limits of accuracy of our data. Measurements of stroke length x_f revealed that the point of piston rebound was generally somewhat closer to the pump tube end wall than predicted by Eq. (4). Figure 8 shows the measured and predicted stroke length as a function of initial pressure ratio across the piston.

The peak pressure at rebound P_{2f} proved to be somewhat lower than predicted. The measured and predicted values of P_{2f}/P_{02} are shown in Fig. 9 as a function of measured piston displacement at rebound. With regard to both stroke length and peak pressure, the primary difference between data and theory appears to be attributable to heat transf during the compression stroke. The compressed gas tempera ures deduced from pressure measurements were as much as 25 percent below the isentropic predictions of Eq. (5). Discrepancies between all of the predicted and measured values decreased as the reservoir pressure was increased and the stroke time was shortened.

Knöös (Ref. 7) investigated the effects of heat transfer from a piston-compressed gas. He found that the heat transfer effects were strongly affected by stroke time. During the compression stroke a thermal boundary layer forms on the walls of the compression tube and the face of the piston. Thus a relatively cool, dense gas layer exists close to the walls. Our isentropic analysis does not account for nonuniform conditions in the compressed

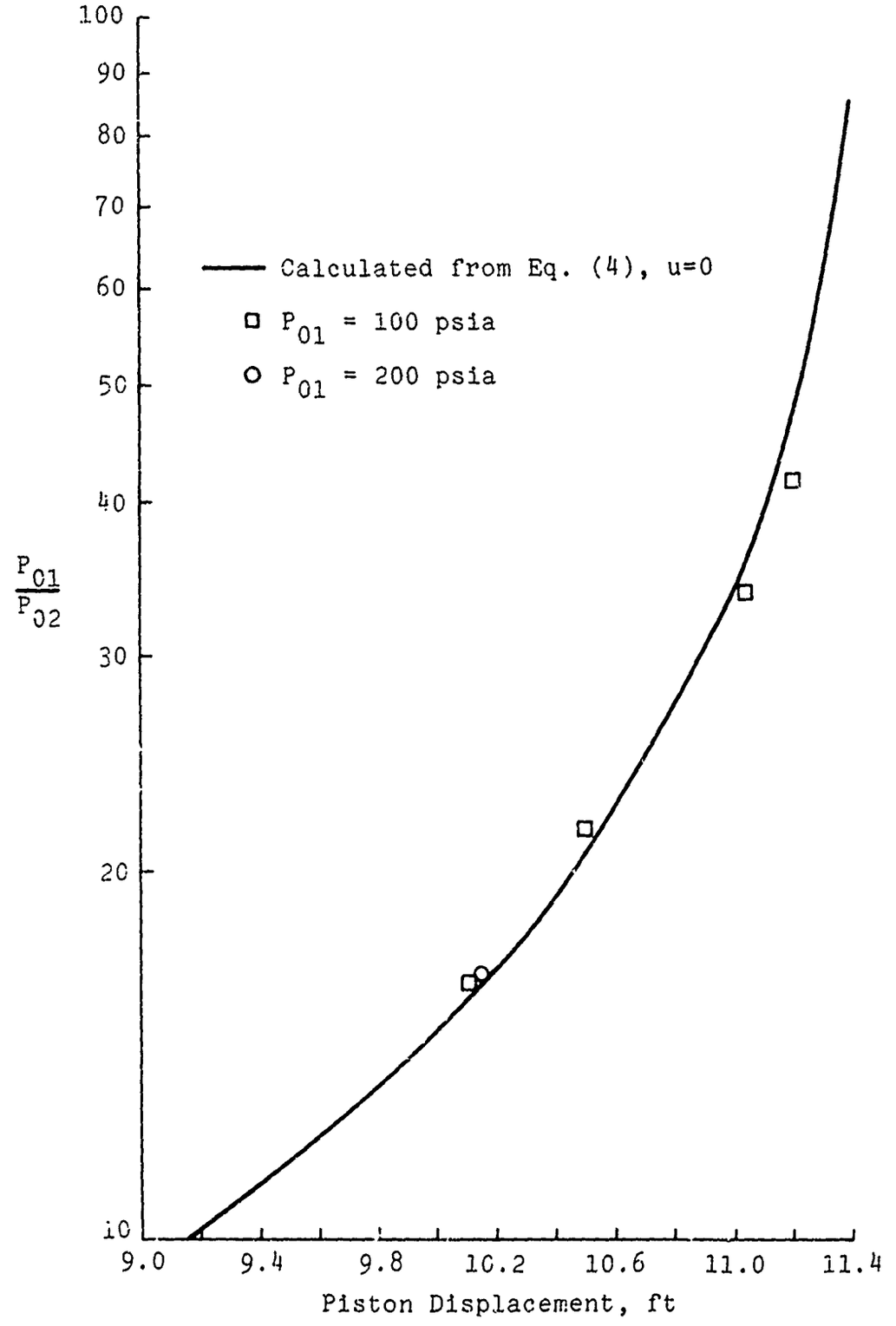

Fig. 8 Initial Pressure Ratio vs Stroke Length

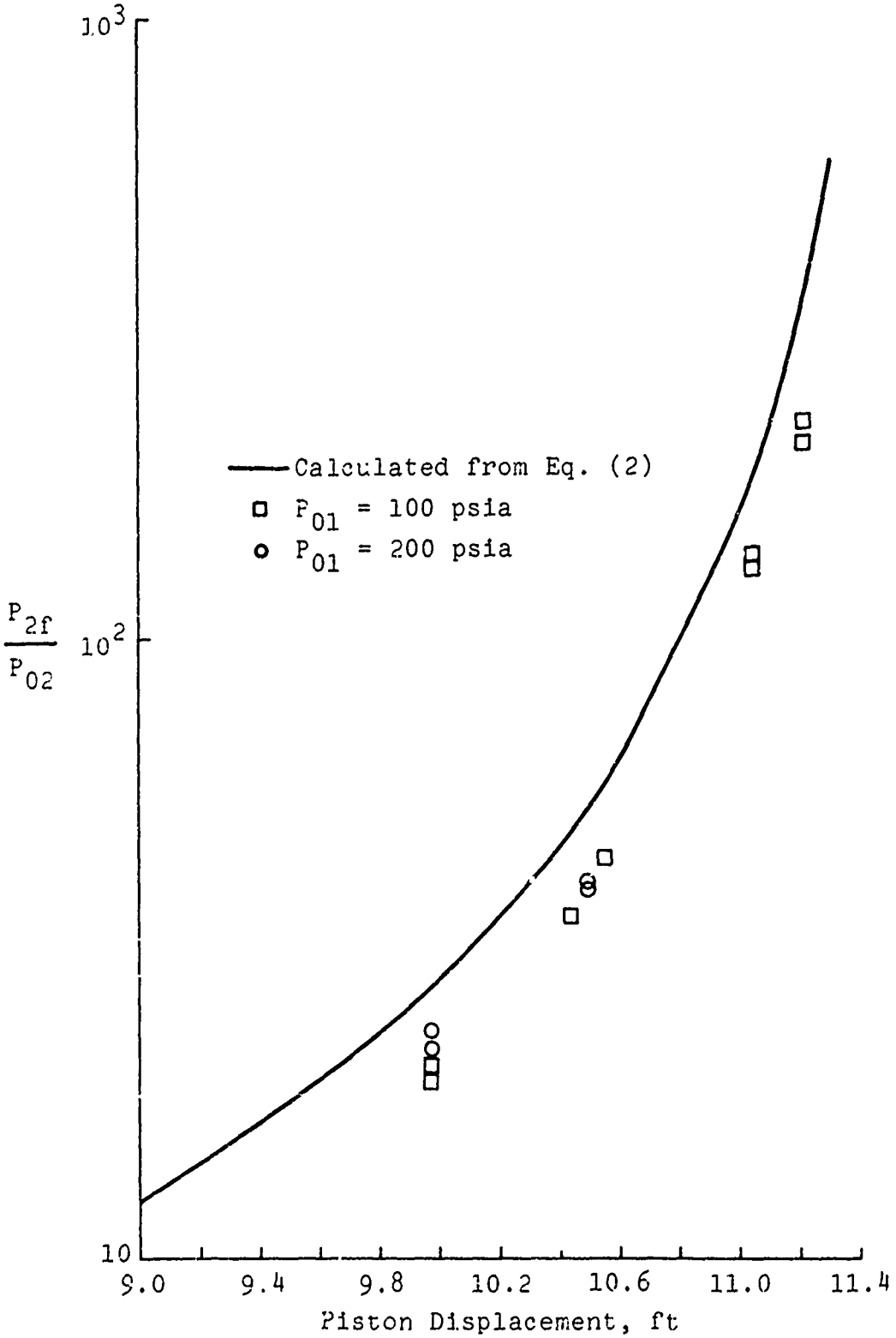

Fig. 9 Compression Ratio vs Stroke Length

gas so it predicts a higher peak pressure than actually exists at rebound.

The gas far from the walls, outside of the thermal boundary layer, should undergo an isentropic compression. As the stroke time is decreased, the thermal boundary layer becomes thinner, and a larger percentage of the driver gas is compressed isentropically. The temperature of this hot core of the compressed gas can be found from the measured ratio of initial to final pressure using the isentropic relation

$$T_{2f} = T_{02} \left(\frac{P_{2f}}{P_{02}}\right)^{\frac{\gamma-1}{\gamma}} . \qquad (12)$$

We have no way of measuring the temperature of the compressed gas directly for comparison with this relation. However, as brought out below, we can estimate the driver temperature by analyzing the driver performance during shock tube operation.

B. Constant Volume Driver

For operation in this mode, the ratio P_{01}/P_{02} is selected so that the piston comes to rest very close to the compressor end wall, and the diaphragm ruptures just at the end of the stroke. Values of P_{2f} and x_f are first measured on a closed tube run. A diaphragm is scribed so as to burst approximately 200 psi higher than P_{2f}. The measured value of x_f is used to size a steel spike that is mounted on the front face of the piston, with its length chosen so that when the piston face arrives at x_f, the tip of the spike will protrude $\frac{1}{4}$-inch through the diaphragm. This method of diaphragm rupture provided very repeatable driver conditions. The driver pressure p_4 was found to be only slightly less than the closed tube maximum pressure P_{2f}.

A series of runs were made with argon in the driven tube to evaluate driver performance for producing shock waves in a heavy gas at high shock Mach numbers. The range of shock Mach numbers in argon should be relatively close to what one would obtain using air as the test gas. Two different driver conditions were chosen, with p_4 = 850 and 1100 psi for a range of initial driven tube pressures p_1, from $\frac{1}{2}$ Torr to 20 Torr. This work was done with 200 psi reservoir pressure, using an early piston design that was considerably heavier (60 pounds) than the hollow one described herein. The shock velocities obtained ranged from 18,000 to over 30,000 feet/second, with a corresponding range of shock Mach numbers from 17 to 30. The microwave traces showed strong attenuation of the shock, particularly for the high velocity tests. A typical microwave trace using argon is shown in Fig. 10. Equal spacing of the resonance peaks would have indicated uniform velocity. Measurements taken from the right side of this trace, corresponding to a physical location close to the driven tube end wall, agreed closely with the velocity obtained from time of arrival at adjacent pressure gauges. The pressure traces showed that for shock velocities greater than 18,000 feet/second the driver length was sufficient for the shock to arrive at the driven tube end wall before arrival of the expansion wave that reflects from the piston face.

A second series of experiments were made with helium in the driven tube to evaluate performance with a light gas, a situation that is of interest for seeded beam experiments. A light gas raised to high energy levels by shock reflection can be seeded with heavier molecules like N_2 or O_2, expanded through a nozzle, and used to produce extremely high velocities of the heavier species for studies of atomic or molecular interactions with species

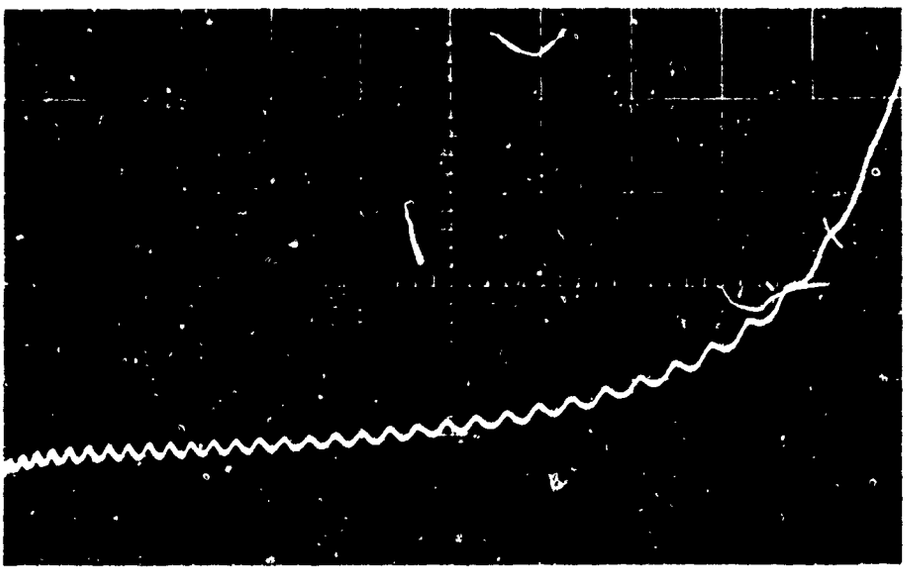

Fig. 10 Signal from Microwave Antenna. Oscilloscope sweep speed 100 microseconds/cm. Resonance peaks occur at 5.8 inch intervals along driven tube.

in the test section. This technique can provide particle velocities considerably higher than a pure heavy gas expansion, and the thermal excitation frozen into the heavy particles during the expansion can be considerably lower.

The new light piston was used for this investigation of shock waves in helium. The shorter stroke time with the lighter piston developed 1320 psi driver pressure using the same compressor conditions that produced 1100 psi with the heavier piston. These driver conditions were used with a range of p_1 from 1 to 60 Torr. The range of shock velocities obtained in helium was about the same as that in argon, but the shock Mach numbers in helium were all less than 8. Sufficient ionization was found behind the incident shock to get well defined microwave traces except at the highest values of p_1. Almost no attenuation of the incident shock in helium was found.

The data obtained using helium as the test gas are shown in Fig. 11 for comparison with shock tube performance predictions. The data are plotted as shock Mach number M_s versus initial diaphragm pressure ratio p_{41}. The curves were predicted by simple shock tube theory (see the appendix), with each curve corresponding to a different assumed helium driver gas temperature. Note that our data falls close to the curve corresponding to a 2000°K driver gas temperature. For comparison, we estimated the driver temperature should have been 2500°K based on the measured compression ratio and the isentropic relation given in Eq. (12). The discrepancy between these two methods of deducing driver gas temperature probably can be attributed to the presence of colder gas in the thermal boundary layer on the walls and on the spike.

Figure 12 shows measurements of the duration of steady pressure in the reflected zone (p_5) plotted as a function of initial

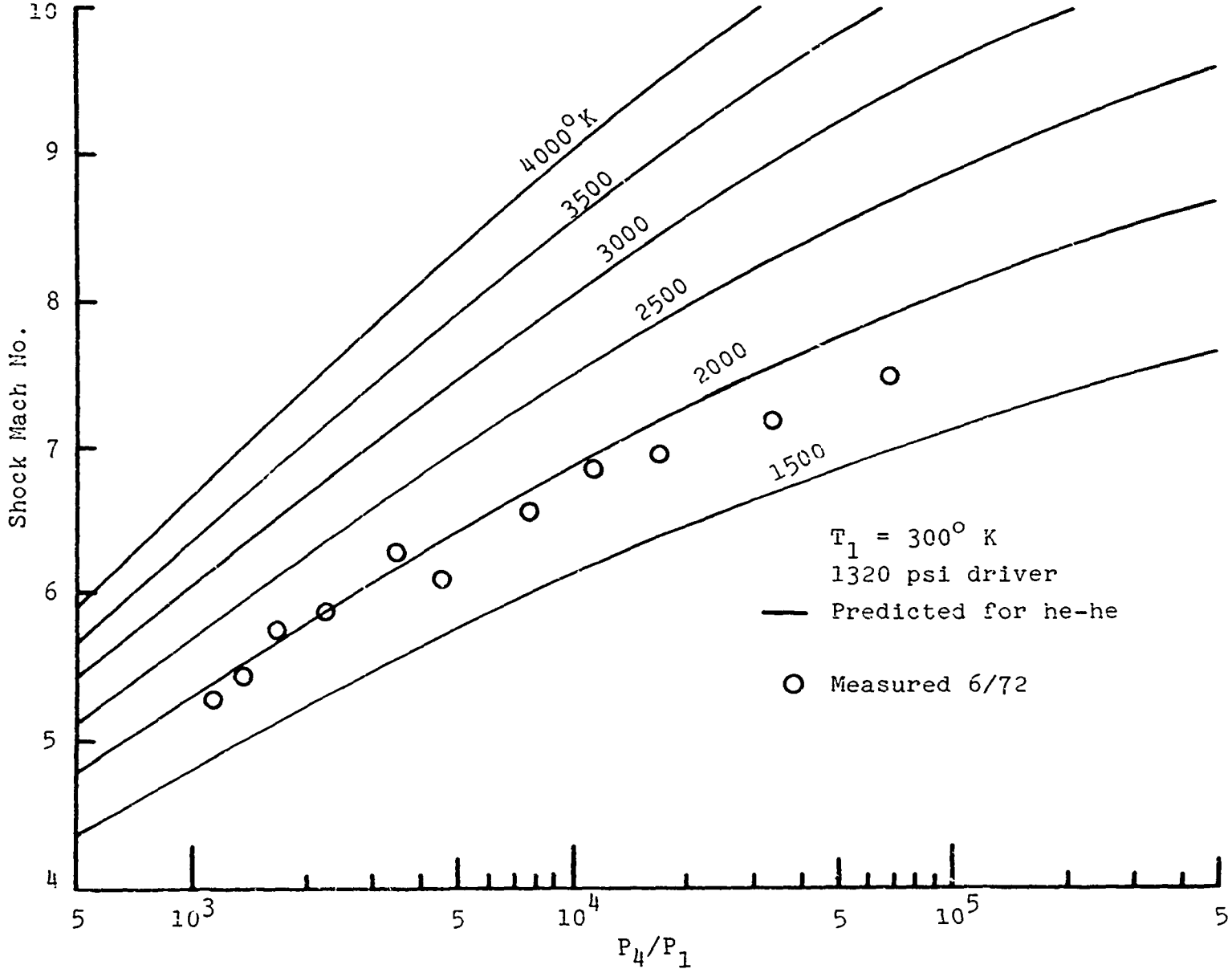

Fig. 11 Performance Characteristics of Constant Volume Driver

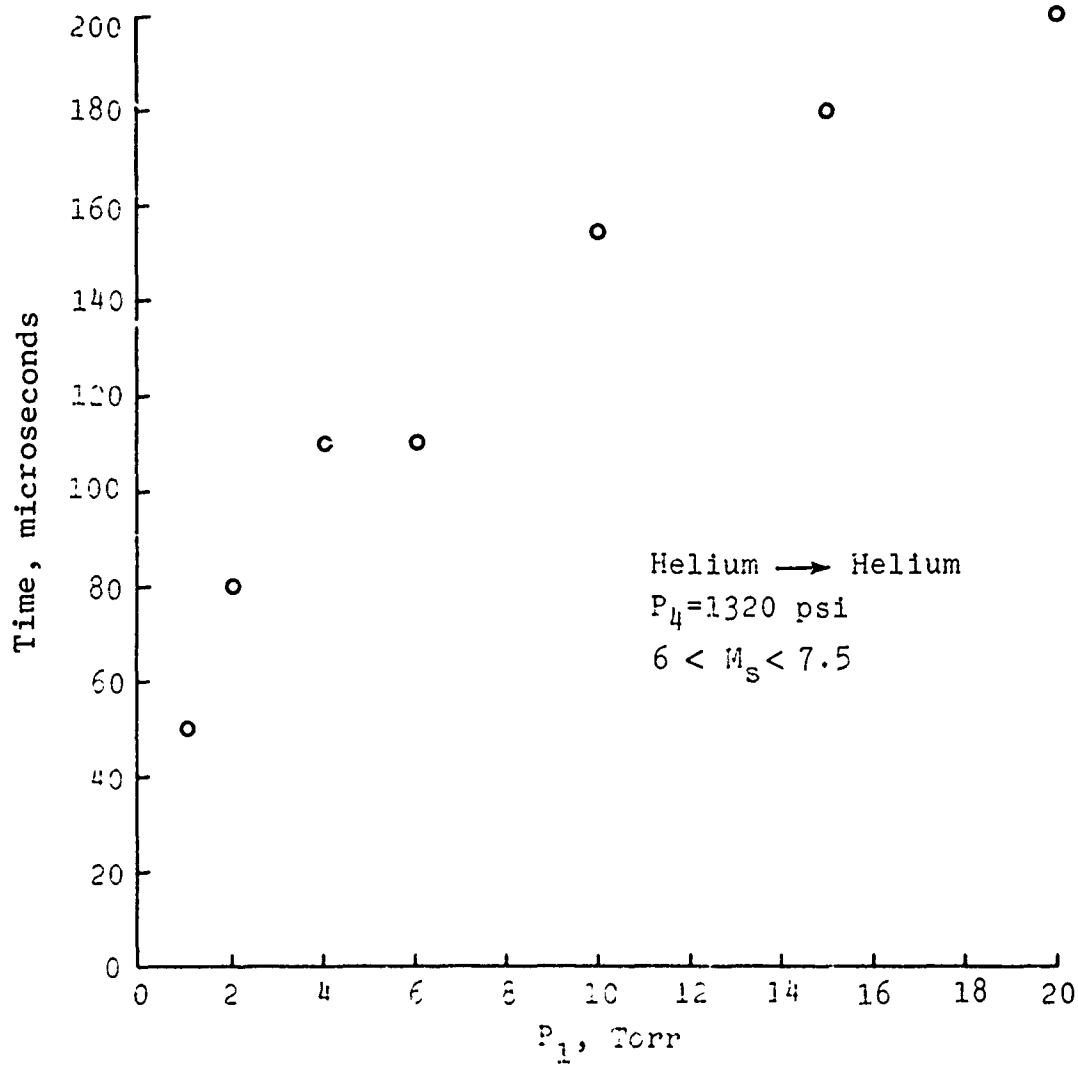

Fig. 12 Region 5 Test Time vs Initial Driven Tube Pressure

driven tube pressure (p_1). Note that at the higher levels of p_1 the conditions in the reflected zone are steady for as long as 200 microseconds. This curve indicates the potential duration of steady flow that would be available if a nozzle were used to expand the shock-heated gas from the reflected zone as in a shock tunnel. It should be noted that the time duration involved in starting a nozzle flow, perhaps a hundred microseconds, must be subtracted from the values shown in the plot. Therefore, at extremely high shock Mach numbers the constant volume technique cannot provide steady stagnation conditions for a sufficient length of time for use in shock tunnel operation.

In summary, it was found that for the constant volume mode, the general range of driver gas temperature was close to the values predicted by isentropic theory based on measurement of the compression ratio, and the driver performance was predictable in terms of conventional shock tube relations. Higher shock velocities could have been produced by increasing p_4 (by as much as a factor of 3) and by decreasing the stroke time to reduce thermal losses during the compression stroke. However the shock velocities obtained were quite high for a system whose initial pressure (P_{01}) was only 200 psi. The factor of seven pressure amplification and the compression heating of the helium driver gas combined to provide an extremely high performance shock tube driver. If air were used in the driven tube, the energy available in the reflected zone would be high enough to produce a very short-duration nozzle flow with velocities up to 30,000 feet/second.

C. Constant Pressure Driver

The difference in driver gas pressure behavior between a constant pressure mode and the constant volume mode described previously

is illustrated by the oscilloscope traces in Fig. 13. The diaphragm rupture point for the latter case (Fig. 13a) is well defined. In contrast, the diaphragm rupture in the constant pressure case (Fig. 13b) occurs somewhere before the maximum pressure point. The pressure remains approximately constant for about 2 milliseconds and then begins a gradual decay.

No spike was used on the piston for the constant pressure experiments; the diaphragm was broken by the pressure rise alone. The diaphragm scribe depth (thus the break pressure) had to be carefully controlled so that the piston would follow a prescribed behavior following diaphragm rupture. Keeping the initial reservoir pressure at 400 psi, and pump tube pressure at 12.5 psi, and using a 2-inch diameter orifice, the driver conditions and piston behavior were controlled by small changes in diaphragm scribe depth. Nominal driver conditions were p_4 = 1000 psi and T_4 = 1500°K.

Several closed tube runs were made for calibration purposes prior to shock tube operation. The stroke time, rebound point, maximum pressure, and pressure history were all quite close to the predicted values. Shock tube runs were then started using a range of driven tube pressures from 10 to 130 Torr to evaluate the driver performance characteristics and to establish the shock Mach number for tailored interface conditions. Argon was used in the driven tube for reasons given below.

The driver and driven tube conditions chosen produced values of M_s between 6 and 12, and the microwave traces showed relatively low attenuation. The data showed that tailored interface conditions were produced at M_s = 10. Pressure data taken during a run at these conditions are shown in Fig. 14a. The upper

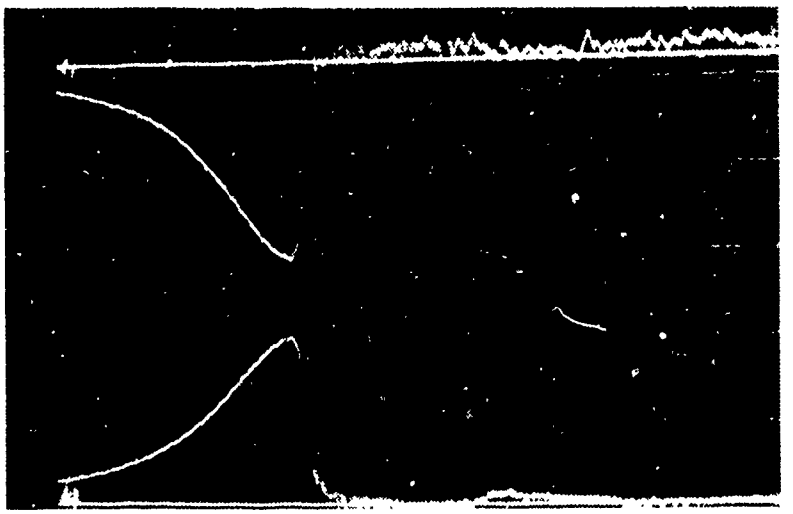

a) Constant Volume Mode; Sweep Speed 2 ms/cm;
Sensitivity Nominally 500 psi/cm

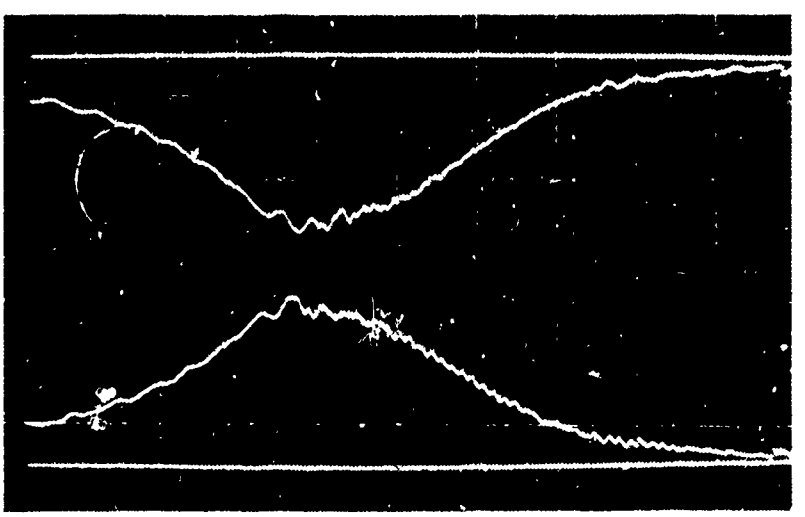

b) Constant Pressure Mode; Sweep Speed 1 ms/cm;
Sensitivity Nominally 500 psi/cm

Fig. 13 Driver Pressure Variation Following Diaphragm Rupture

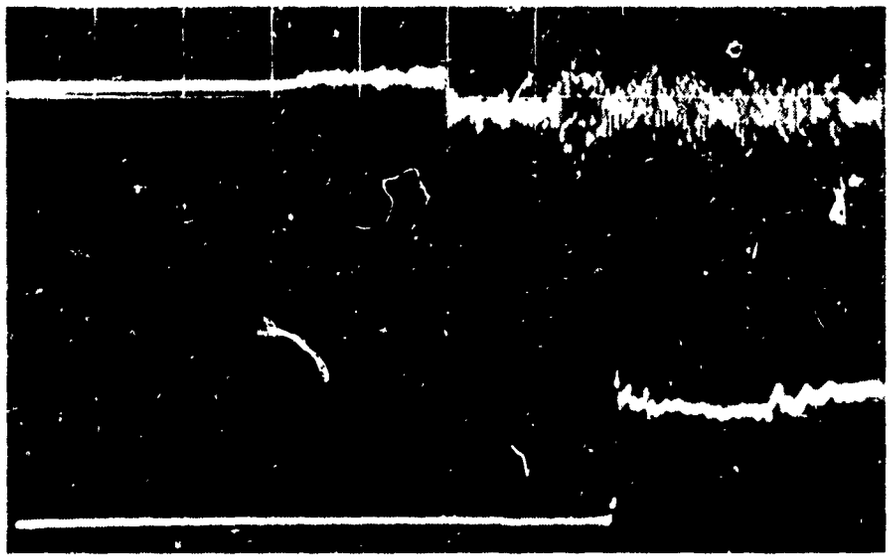

a) Pressure Record; Upper Beam Sensitivity 100 psi/cm; Lower Beam 200 psi/cm; Sweep Speed 0.2 ms/cm

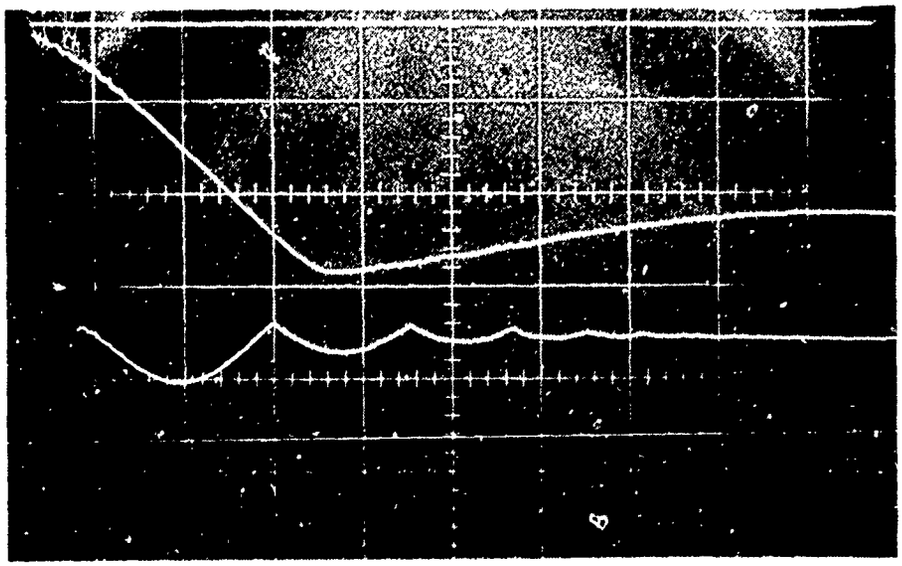

b) Recoil Traces; Tube Displacement at 0.5 in./cm; Upper Beam Sweep Speed 10 ms/cm, lower beam 50 ms/cm.

Fig. 14 Shock Tube Operation with Constant Pressure Driver

trace shows incident shock arrival at an upstream pressure gauge; the lower trace shows incident and reflected shock pressures at a point $\frac{1}{2}$-inch from the driven tube end wall. The duration of steady p_5 was at least 1 millisecond. The noise observed on these signals prior to shock arrival, most noticeable on the upper beam, was generated by impact of the diaphragm leaves. The disturbances moved fast enough to outrun the shock during these tests, but were not observed during the higher velocity tests described in Section V-B.

The steady conditions in the reflected zone are ended by arrival of an expansion wave generated by deceleration of the piston at the end of its stroke. The piston behavior during this type of driver operation is displayed in the tube recoil trace in Fig. 14b. The downward displacement of the upper beam and upward displacement of the lower beam relative to their base lines are each proportional to the distance traveled by the piston after launch, but the signals are displayed at different beam sweep speeds. The portion of the upper beam up to the maximum displacement point describes the compression stroke, and from it we can determine the maximum piston velocity, the stroke time, and the stroke length. On this run the piston passed through a maximum velocity of 380 feet/second and decelerated to about 240 feet/second at diaphragm rupture. The diaphragm rupture point is not apparent on this trace, but it occurred about 5 milliseconds before the first signal peak.

The first maximum in the signal occurred when the piston came to rest about an inch from the compressor end wall and rebounded because the pressure of residual gas ahead of the piston was greater than that of the expanded reservoir gas. This rebound carried the piston a few feet back from the end wall, it reversed direction, and as shown by the lower beam this time it struck the end wall because the gas ahead of it had sufficient time to cool. This initial

impact was followed by several additional impacts on this run because of the pneumatic plungers (described in Section VI) on the end wall used for impact absorbtion. With the exception of the repeated end wall impact, this piston behavior was observed in all of our constant pressure type runs.

D. Comparison of Two Driver Modes

The shock tube performance characteristics of a constant volume driver, illustrated in Fig. 11, are generated by relations that are well known (Ref. 8) because most shock tube drivers operate in this mode. The relations required for such calculations are presented in the appendix. The method used to predict the performance of a constant pressure driver is somewhat more complex than the constant volume case and not currently as well defined. The method developed to predict constant pressure driver performance is also presented in the appendix. In addition, the appendix also presents our method for calculating the shock Mach number required for tailored interface operation (M_{st}) as a function of driver gas temperature. The relation between M_{st} and p_4 is different for a constant pressure driver than for a constant volume driver.

Figure 15 shows curves of M_s versus the initial diaphragm pressure ratio p_{41} for different assumed values of T_4. These curves were generated for a constant pressure helium driver with argon in the driven tube using the method outlined in the appendix. They are valid for the specific case of our tube geometry with a 2-inch diameter orifice at the diaphragm station. The data shown were obtained during runs described in the previous section. Agreement between data and theory is close enough to justify use of our analysis for predicting shock tube characteristics and to verify the value of driver gas temperature at diaphragm rupture

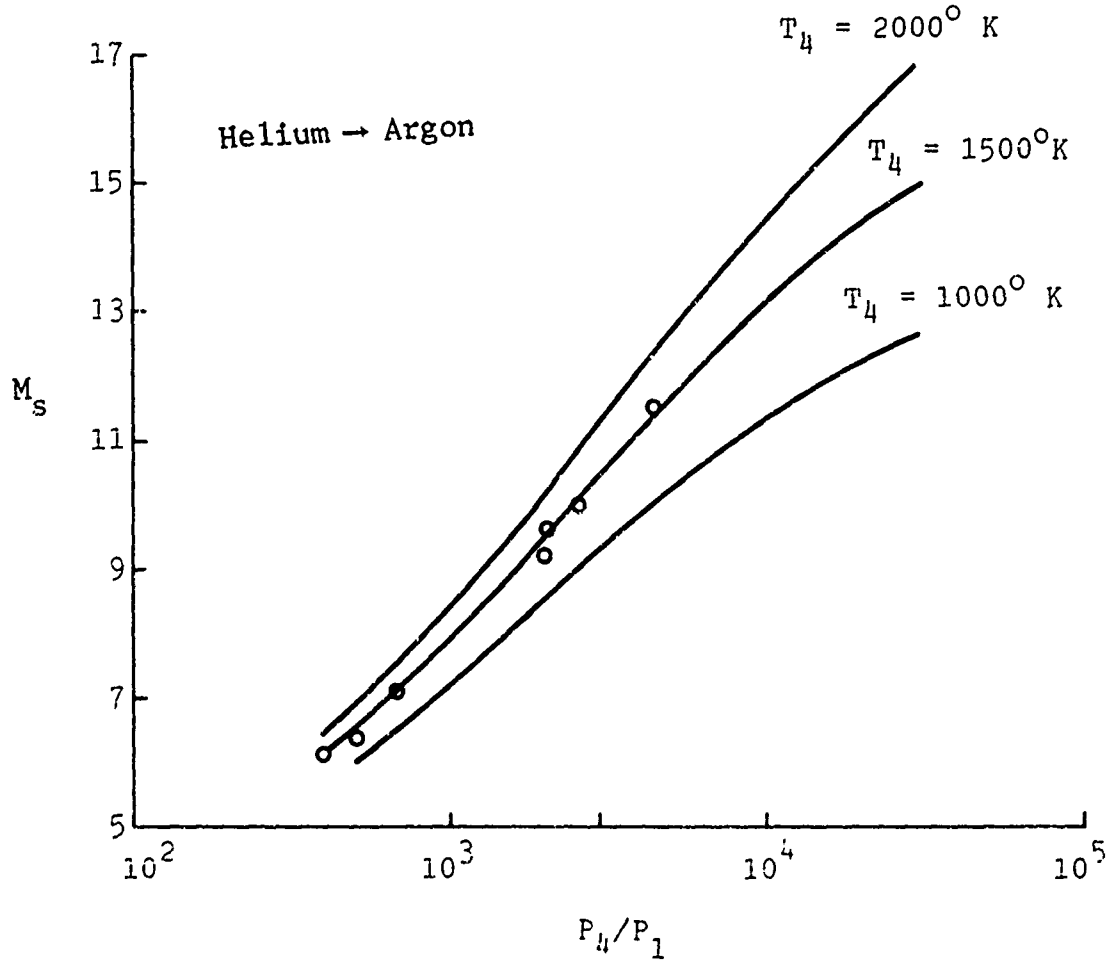

Fig. 15 Performance Characteristics of a Constant Pressure Driver with a 2-Inch Diameter Orifice

predicted by our computer program. The improvement in performance that could be obtained by increasing the orifice diameter to three inches is shown by the curves in Fig. 16.

Figure 17 shows the advantages of using the constant pressure mode. Curves of the tailoring shock Mach number M_{st} versus driver gas temperature T_4 are presented for both a constant pressure driver and for a constant volume driver. Both curves were computed assuming helium in the driver and argon in the driven tube. The constant pressure curve was developed using a method presented in the appendix, and is independent of the orifice diameter chosen to produce the flow. The constant volume curve was developed from relations presented in Ref. 9. Comparison of these curves shows that for a given driver gas temperature the constant pressure driver will provide tailored interface operation at a higher shock Mach number and thus provide greater energy for a nozzle expansion from the reflected shock zone. As pointed out in the appendix, the higher M_{st} obtained with the constant pressure driver comes about because of differences between unsteady and steady-state driver gas expansions. Thus a constant pressure driver would be expected to have a similar advantage for other driver-driven gas combinations.

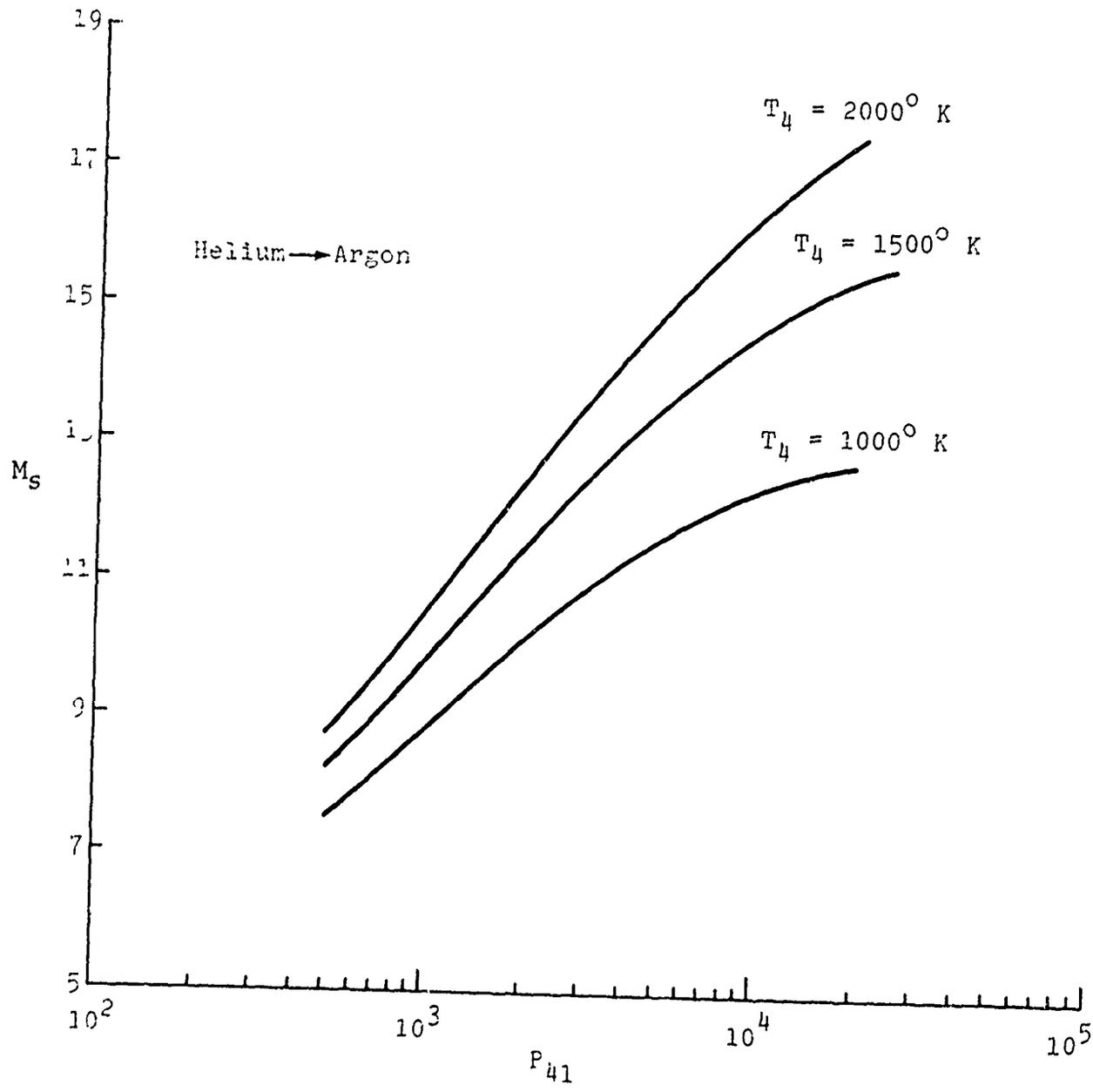

Fig. 16 Performance Characteristics of Constant Pressure Driver With a 3-Inch Diameter Orifice

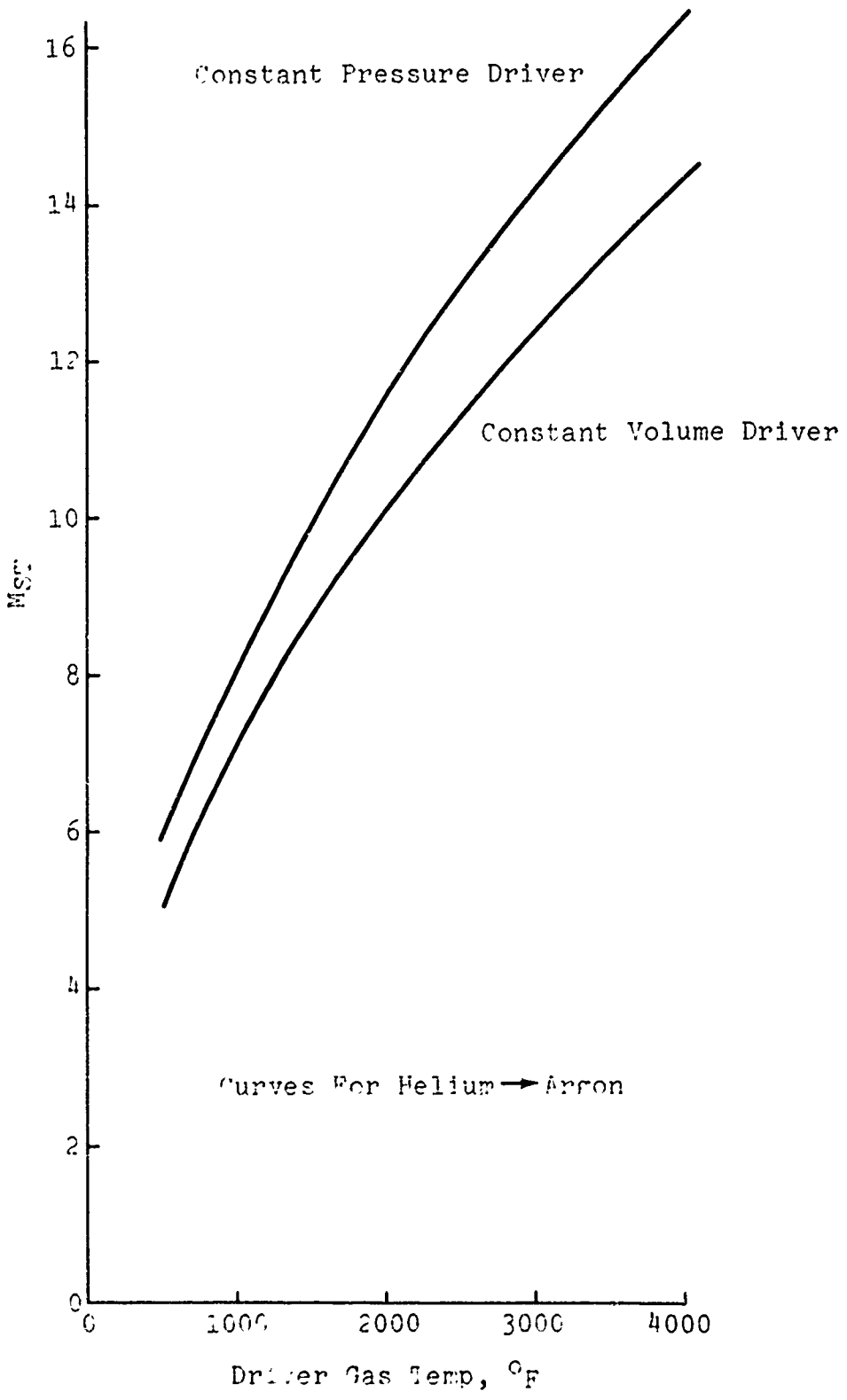

Fig. 17 Shock Mach Number for Tailored Interface Operation as a Function of Driver Gas Temperature

VI. CONCLUSIONS

The free-piston compressor produces high energy shock tube driver conditions in two different modes of operation. The constant volume mode produces maximum energy in the reflected zone at the end of the driven tube for a few hundred microseconds; the constant pressure mode produces a longer duration of steady reflected zone pressure at a somewhat reduced energy level. Measurements showed that piston behavior and compressed gas conditions were adequately predicted by the analyses described herein. Measurements of shock driving characteristics and tailoring shock Mach number that were taken during operation in the constant pressure mode were found to be predictable by methods developed in this report.

Based on this investigation we conclude that tailored interface operation should be possible at shock Mach numbers up to 15 in air, and off-tailored operation should extend above $M_s = 30$. Strong shock attenuation should be expected at the higher values of M_s, but this may be reduced by honing the walls of the driven tube. Some design work remains to be done before attempting to develop a flow from the reflected zone into a vacuum chamber. The support system presently used must be redesigned to permit free recoil with the end of the driven tube inside a vacuum tank. An adequate sliding seal at the tube-tank interface is required. In addition, for safety purposes, we would recommend that the present manually operated high pressure valves be replaced by remotely activated valves that can be interlocked to the piston release mechanism.

One advantage of piston compression for driver gas production is that the diaphragm is broken by a momentary surge of high energy

gas that has a pressure far in excess of the initial pressure anywhere in the system. Operation in the constant pressure mode permits use of an extremely small driver volume and for tailored interface work its performance is equivalent to a much longer conventional driver that would require almost an order of magnitude more energy input.

VII. REFERENCES

1. Williard, J. W., "Design and Performance of the JPL Free-Piston Shock Tube," Proceedings of the Fifth Hypervelocity Techniques Symposium, March 1967.

2. Stalker, R. J., "Characteristics of the Free-Piston Shock Tube," Proceedings of the Fifth Shock Tube Symposium, April 1965.

3. Stalker, R. J., "A Study of the Free-Piston Shock Tunnel," AIAA Journal, December 1967.

4. Stoddard, F. J., "Theoretical and Experimental Studies of Piston-Compressor Techniques for Producing Hypervelocity Test Flows," AIAA Fourth Aerodynamic Testing Conference, Paper No. 69-334, April 1969.

5. Flagg, R. F., Detailed Analysis of Shock Tube Tailored Conditions, Technical Memorandum RAD-TM-63-64, Research and Advanced Development Division, AVCO Corporation, Wilmington, Massachusetts, 30 September 1963.

6. Roffe, G. A., The Free Piston Shock Tube Driver: A Preliminary Theoretical Study, Technical Report No. 32-560, Jet Propulsion Laboratory, Pasadena, California, December 15, 1963.

7. Knöös, S., "Theoretical and Experimental Study of Piston Gas-Heating with Laminar Energy Losses," AIAA Journal, November 1971.

8. Glass, I. I. and Hall, J. G., Handbook of Supersonic Aerodynamics, Section 18, Shock Tubes, NAVORD Report 1488, Vol. 6, December 1959.

9. Loubsky, W. J. and Reller, J. O. Jr., Analysis of Tailored Interface Operation of Shock Tubes with Helium-Driven Planetary Gases, NASA TN D-3495, July 1966.

APPENDIX

PREDICTION OF SHOCK TUBE PERFORMANCE CHARACTERISTICS

The shock velocity produced by a given set of driver and driven tube conditions can be predicted once the nature of the driver gas expansion and the tube geometry have been specified. The performance of a shock tube driver is characterized by the variation of shock Mach number with initial diaphragm pressure ratio at different driver gas temperatures. Such performance characteristics are well known for a conventional constant volume shock tube driver, but are not readily available for a constant pressure driver. The equations governing the performance of both types of drivers presented below show that the difference in their performance comes about because in one case the driver gas undergoes an unsteady expansion into the driven tube, while in the other case it undergoes a steady-state expansion. It is also shown that, because of the difference between an unsteady expansion and a steady-state expansion, tailored interface conditions are obtained at higher M_s in a constant pressure driver than in a constant volume driver with the same initial conditions for both.

Prediction of M_s for Given p_{41} and T_4

In either mode of driver operation, the shock velocity produced by a given set of driver conditions is found by matching the conditions behind the shock front to the conditions behind the interface in the expanded driver gas. For both modes, the boundary condition for this match is that the pressure and the velocity of flow must be the same on both sides of the interface.

The two modes of operation are illustrated in Figs. A-1 and A-2. Standard shock tube notation is used in Fig. A-1. The notation and the physical model illustrated in Fig. A-2 follow that used by Russell[†] in an investigation of the influence of a flow constriction at the diaphragm station on shock tube behavior. Russell found that the assumption of a stationary Fanno recompression downstream of the orifice provided better agreement with his data than an alternate model based on normal shock recompression. The Fanno process is assumed to take place at constant area downstream of the orifice. Energy and mass flow are conserved through this region but momentum is dissipated by an unspecified mechanism.

For both modes of driver operation the conditions in Region 2 are found from the normal shock relations. Applying the boundary condition of equal pressure and velocity across the interface

$$u_3 = u_2 = \frac{2a_1}{\gamma_1 + 1}\left(M_s - \frac{1}{M_s}\right) \tag{A-1}$$

$$p_3 = p_2 = p_1\left[\frac{2\gamma_1 M_s^2 - (\gamma_1 - 1)}{\gamma_1 + 1}\right] \tag{A-2}$$

where $M_s = u_s/a_1$. Values of u_3 and p_3 also can be computed directly from the conditions in Region 4 once the nature of the driver gas expansion has been specified. The M_s corresponding to given driver conditions is that value of M_s that satisfies both the normal shock relations above and the equations governing the driver gas expansion to Region 3. For the constant volume

[†]Russell, D. A., A Study of Area Change Near the Diaphragm Station of a Shock Tube, Memorandum No. 57, Gugenheim Aeronautical Laboratory, California Institute of Technology, July 20, 1960.

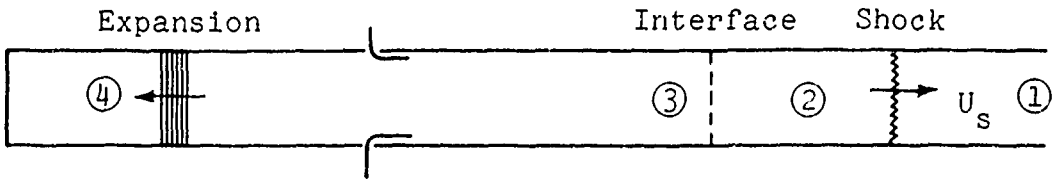

Fig. A-1 Constant Volume Driver Expansion

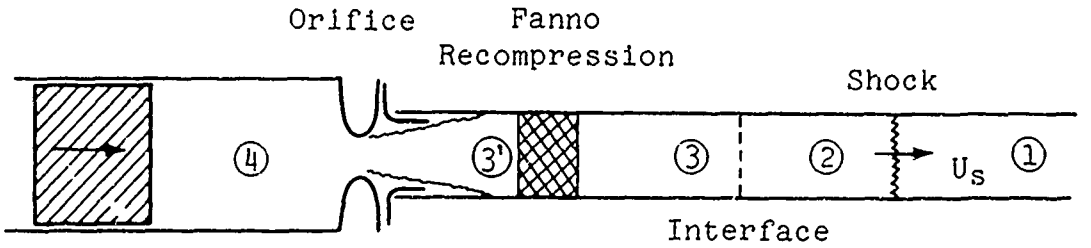

Fig. A-2 Constant Pressure Driver Expansion

driver this solution can be obtained in analytic form. For the constant pressure driver one must iterate to find M_s.

The equations governing driver gas expansion are shown below. For simplicity we have assumed that both driver and driven gases are perfect, with isentropic exponents γ_4 and γ_1, respectively. For our work this assumption is probably quite good for the helium driver gas. For the gas in the driven tube, however, Eqs. (A-1) and (A-2) can be significantly in error at high values of M_s. For our experimental work this error was minimized by using monatomic gases in the driven tube. The normal shock pressure ratio is not strongly influenced by real gas effects in a monatomic gas. Comparison with calculations that account for real gas effects showed that even at the higher shock Mach numbers the value of p_2/p_1 computed from Eq. (A-2) was only a few percent high. This level of accuracy is sufficient for estimating performance characteristics with a monatomic gas, but real gas effects would have to be considered if a diatomic gas were chosen in the driven tube.

Case I - Constant Volume Driver Expansion

It has been shown (Ref. 8) that the equation for velocity change across an unsteady expansion

$$a_4 = a_3 + \frac{(\gamma_4 - 1)}{2} u_3 \qquad \text{(A-3)}$$

can be combined with the isentropic relation

$$\frac{p_4}{p_3} = \left(\frac{a_4}{a_3}\right)^{\frac{2\gamma_4}{\gamma_4 - 1}} \qquad \text{(A-4)}$$

and the normal shock relations above to yield

$$p_{41} = \frac{p_4}{p_1} = \frac{2\gamma_1 M_1^2 - (\gamma_1 - 1)}{\gamma_1 + 1} \left[1 - \frac{\gamma_4 - 1}{\gamma_1 + 1} \left(\frac{a_1}{a_4} \right) \left(M_s - \frac{1}{M_s} \right) \right]^{\frac{-2\gamma_4}{\gamma_4 - 1}} \qquad \text{(A-5)}$$

Figure 11 shows a plot of M_s versus p_{41} obtained from this relation for different values of T_4 assuming helium in both the driver and driven tubes.

Case II - Constant Pressure Driver Expansion

In this case the geometry near the diaphragm station must be carefully defined. As shown in Fig. A-1, the driver gas expands isentropically from Region 4 to Region 3' and then undergoes a compression between Regions 3' and 3. The tube cross-sectional areas in Region 4, in Region 3, and at the orifice must be specified to find a solution. Assuming steady-state, isentropic flow of the driver gas into the driven tube, we can use one dimensional flow relations to define M_4 and $M_{3'}$ from the area ratios between these sections and the sonic region. Thus the conditions in Region 3' can be found from the conditions in Region 4. Following Russell, we assume that the supersonic flow in Region 3' then undergoes a Fanno recompression to the conditions in Region 3. Russell has shown that conservation of energy and mass across this recompression can be used to relate the change in velocity to the change in pressure between Regions 3' and 3. Stalker presents this relation in the form

$$\frac{p_3}{p_{3'}} = \frac{u_{3'}}{u_3} \left\{ 1 + \frac{\gamma_4 - 1}{2} M_{3'}^2 \left[1 - \left(\frac{u_3}{u_{3'}} \right)^2 \right] \right\} \qquad \text{(A-6)}$$

To find M_s for given driver conditions we developed an iterative procedure based on Eqs. (A-1), (A-2), (A-6), and the

equations of isentropic flow for the driver gas. The results of such calculations are shown in Figs. 15 and 16 for orifice diameters of 2 and 3 inches. Curves of M_s versus p_{41} are shown for different values of T_4 assuming helium driver gas and argon in the driven tube.

Prediction of Tailoring Shock Mach Number

Tailored interface conditions exist in the reflected zone when the reflected shock passes through the interface without generating any secondary waves that reflect back toward the closed end of the tube. In the analysis which follows we consider only the case where $\gamma_4 = \gamma_1$, and assume both gases are perfect. In this case tailored conditions exist when $a_2 = a_3$. We further simplify our analysis by considering only the special case of a helium driver with argon in the driven tube. Then reflected zone conditions will be tailored when

$$T_2 = 10\, T_3 \quad . \tag{A-7}$$

Both T_2 and $u_3 = u_2$ can be found from the normal shock relations for a given value of M_s. T_3 can be related to T_4 by specifying the nature of the driver gas expansion. This relation determines M_{st} as a function of T_4 and has a different form for a constant pressure driver than for a conventional constant volume driver. A constant volume driver is governed by Eq. (A-3) for an unsteady expansion. A constant pressure driver is governed by the steady-state energy equation

$$h_4 = h_3 + \frac{u_3^2}{2} \tag{A-8}$$

where the enthalpy h is proportional to temperature for a perfect gas.

Figure 17 shows a plot of M_{st} versus T_4 for these two different types of driver gas expansions. The curve representing the constant pressure driver is not dependent on orifice diameter. Note that for a given value of T_4 the constant pressure driver will provide tailored conditions at a higher value of M_{st}. The reason can be seen by comparing Eqs. (A-3) and (A-8). For given T_4 and u_3, one obtains a higher value of T_3 with a steady-state expansion, and thus must increase M_s in order to satisfy Eq. (A-7). For this reason one would expect that regardless of what driven tube gas was chosen the constant pressure driver would provide a higher value of M_{st} than could be obtained with the conventional constant volume driver.